NASA TECHNICAL NOTE

NASA TN D-6997

NASA TN D-6997

SHOCK WAVES AND DRAG IN THE NUMERICAL CALCULATION OF ISENTROPIC TRANSONIC FLOW

by Joseph L. Steger and Barrett S. Baldwin

Ames Research Center
Moffett Field, Calif. 94035

NATIONAL AERONAUTICS AND SPACE ADMINISTRATION • WASHINGTON, D. C. • OCTOBER 1972

1. Report No.	2. Government Accession No.	3. Recipient's Catalog No.
NASA TN D–6997		

4. Title and Subtitle	5. Report Date
SHOCK WAVES AND DRAG IN THE NUMERICAL CALCULATION OF ISENTROPIC TRANSONIC FLOW	October 1972
	6. Performing Organization Code

7. Author(s)	8. Performing Organization Report No.
Joseph L. Steger and Barrett S. Baldwin	A-4519
	10. Work Unit No. 136-13-05-08-00-21
9. Performing Organization Name and Address	11. Contract or Grant No.
NASA-Ames Research Center Moffett Field, Calif., 94035	
	13. Type of Report and Period Covered
12. Sponsoring Agency Name and Address	Technical Note
National Aeronautics and Space Administration Washington, D. C. 20546	14. Sponsoring Agency Code

15. Supplementary Notes

16. Abstract

Properties of the shock relations for steady, irrotational, transonic flow are discussed and compared for the full and approximate governing potential equations in common use. Results from numerical experiments are presented to show that the use of proper finite difference schemes provide realistic solutions and do not introduce spurious shock waves. Analysis also shows that realistic drags can be computed from shock waves that occur in isentropic flow. In analogy to the Oswatitsch drag equation, which relates the drag to entropy production in shock waves, a formula is derived for isentropic flow that relates drag to the momentum gain through an isentropic shock. A more accurate formula for drag based on entropy production is also derived, and examples of wave drag evaluation based on these formulas are given and comparisons are made with experimental results.

17. Key Words (Suggested by Author(s))	18. Distribution Statement
Transonic flow Wave drag Shock waves	Unclassified - Unlimited

19. Security Classif. (of this report)	20. Security Classif. (of this page)	21. No. of Pages	22. Price*
Unclassified	Unclassified	45	$3.00

* For sale by the National Technical Information Service, Springfield, Virginia 22151

NOMENCLATURE

A	shock surface area
a	speed of sound
C_D	drag coefficient
c	airfoil chord
D	drag force
F	function defined by equation (19)
f	surface of integration
G	function defined by equation (29)
h	fluid enthalpy
i	isentropic
M	Mach number
M_{crit}	Mach number at which sonic flow is reached
n	normal distance
P	function defined by equation (23)
p	fluid pressure
q	fluid velocity
R	gas constant
r	Mach number function defined by equation (22) or equation (C3)
s	specific entropy
T	fluid temperature
u	$\frac{q_x}{a_{st}}$
v	$\frac{q_y}{a_{st}}$
x	x coordinate

y	y coordinate
δ	wedge angle or flow deflection angle
γ	ratio of specific heats
θ	angle between shock line and x axis
ρ	fluid density
τ	airfoil thickness ratio

Subscripts

1	ahead of shock
2	behind shock
∞	free stream
crit	sonic velocity condition
i	isentropic
n	normal component
RH	Rankine-Hugoniot flow
st	stagnation
x	x component
y	y component

SHOCK WAVES AND DRAG IN THE NUMERICAL CALCULATION OF ISENTROPIC TRANSONIC FLOW

Joseph L. Steger and Barrett S. Baldwin

Ames Research Center

SUMMARY

Properties of the shock relations for steady, irrotational, transonic flow are discussed and compared for the full and approximate governing potential equations in common use. Results from numerical experiments are presented to show that the use of proper finite difference schemes provide realistic solutions and do not introduce spurious shock waves. Analysis also shows that realistic drags can be computed from shock waves that occur in isentropic flow. In analogy to the Oswatitsch drag equation, which relates the drag to entropy production in shock waves, a formula is derived for isentropic flow that relates drag to the momentum gain through an isentropic shock. A more accurate formula for drag based on entropy production is also derived, and examples of wave drag evaluation based on these formulas are given and comparisons are made with experimental results.

INTRODUCTION

Finite difference procedures using both time-dependent formulations and relaxation methods have been developed to compute the steady, inviscid, transonic flow about arbitrary bodies. In most of these techniques the flow is assumed to be adiabatic and irrotational – that is, isentropic – and shock waves, if they appear at all, are not strong. The assumption that the flow is isentropic leads to considerable savings in computer algebra and storage, and for these reasons of efficiency, the isentropic assumption is quite useful in numerical computation. However, the implications of this assumption in transonic flow are perhaps not fully appreciated. For example, even though the flow is assumed to be isentropic, wave drag arising from shock "losses" can be evaluated. This seemingly contradictory result occurs because the isentropic shock relations – the permissible weak solutions (Lax, ref. 1) to the isentropic flow equations – do not conserve momentum in the direction normal to the shock.

Current relaxation procedures developed to treat transonic flow also require the isentropic assumption. Both time-dependent, finite-difference techniques and current relaxation procedures allow isentropic shock waves to evolve naturally without the explicit use of sharp shock conditions. Unlike the time-dependent schemes, the relaxation procedures do not attempt to follow characteristics in time in order to automatically maintain the proper domain of dependence. Instead, "proper" hyperbolic or elliptic difference formulas must be used, depending on whether the flow is subsonic or supersonic. However, while the concept of proper differencing in transonic flow has been extensively used since Murman and Cole's first successful exploitation of the idea (ref. 2), it has not been fully explored.

Both the concept of drag in an isentropic flow and the concept of shock formation can be studied under guidelines suggested by the theory of weak solutions. Consequently, this paper begins with the study of the isentropic shock relations as predicted by this theory. Several numerical experiments are reported for the relaxation methods which demonstrate that the differencing technique is general and can give all possible solutions. A major portion of this paper is devoted to a detailed analysis of the drag mechanism in isentropic flow. From this analysis, a practical method is developed for the evaluation of wave drag which does not require integration of surface pressures. Results from this technique are also presented.

WEAK SOLUTIONS FOR TRANSONIC FLOW EQUATIONS

Consider the equations of irrotational, inviscid, adiabatic flow for a perfect gas in two dimensions

$$\frac{\partial \rho q_x}{\partial x} + \frac{\partial \rho q_y}{\partial y} = 0 \tag{1a}$$

$$\frac{\partial q_x}{\partial y} - \frac{\partial q_y}{\partial x} = 0 \tag{1b}$$

$$h_{st} = \text{constant} \tag{1c}$$

$$s = \text{constant} \tag{1d}$$

Equations (1a) through (1d) may be combined with the equation of state of a calorically perfect gas to obtain two equations for the two dependent variables, the velocity components u and v

$$\frac{\partial}{\partial x}\left\{\left[1 - \frac{\gamma-1}{2}(u^2+v^2)\right]^{\frac{1}{\gamma-1}} u\right\} + \frac{\partial}{\partial y}\left\{\left[1 - \frac{\gamma-1}{2}(u^2+v^2)\right]^{\frac{1}{\gamma-1}} v\right\} = 0 \tag{2}$$

$$\frac{\partial u}{\partial y} - \frac{\partial v}{\partial x} = 0 \tag{3}$$

where

$$u \equiv q_x/a_{st}, \quad v \equiv q_y/a_{st}$$

According to the theory of a weak solution (Lax, ref. 1, and Lomax, Kutler and Fuller, ref. 3) for hyperbolic systems, solutions of equations (2) and (3) may be discontinuous across a smooth curve (which may be a shock wave) and constitute a weak solution if they satisfy the relations

$$\tan\theta \left\{ \left[1 - \frac{\gamma-1}{2}\left(u_1^2 + v_1^2\right)\right]^{\frac{1}{\gamma-1}} u_1 - \left[1 - \frac{\gamma-1}{2}\left(u_2^2 + v_2^2\right)\right]^{\frac{1}{\gamma-1}} u_2 \right\}$$

$$= \left\{ \left[1 - \frac{\gamma-1}{2}\left(u_1^2 + v_1^2\right)\right]^{\frac{1}{\gamma-1}} v_1 - \left[1 - \frac{\gamma-1}{2}\left(u_2^2 + v_2^2\right)\right]^{\frac{1}{\gamma-1}} v_2 \right\} \tag{4}$$

and

$$\left(u_1 - u_2\right) = -\tan\theta \left(v_1 - v_2\right) \tag{5}$$

Here θ is the angle between the shock wave and the x axis, while the subscripts 1 and 2 indicate values before and behind the shock wave. Note that equations (4) and (5) permit a continuous solution, $u_1 = u_2$ and $v_1 = v_2$, as well as the discontinuous solution. Equations (4) and (5) pertain to isentropic flow and admit solutions analogous to the Rankine-Hugoniot relations.

The discontinuous solution of the flow conservation equations of mass, momentum, and energy[1] is given by the Prandtl relation, but a corresponding exact closed-form, discontinuous solution of equations (4) and (5) has not been found. Across a normal shock, equations (4) and (5) reduce to

$$\left(1 - \frac{\gamma-1}{2} u_1^2\right)^{\frac{1}{\gamma-1}} u_1 = \left(1 - \frac{\gamma-1}{2} u_2^2\right)^{\frac{1}{\gamma-1}} u_2 \tag{6}$$

while for Rankine-Hugoniot flow the Prandtl relation for a normal shock is

$$u_1 u_2 = \frac{2}{\gamma+1} \tag{7}$$

---

[1] Here the flow described by these equations is referred to as Rankine-Hugoniot flow. In Rankine-Hugoniot flow, entropy is not conserved across a shock plane, and the Rankine-Hugoniot equations are satisfied across any arbitrary plane in the field. An alternate flow, for example, could be described by the conservation equations of mass and momentum (the Euler equations) and conserve entropy in place of energy across a shock wave.

A numerical evaluation of equation (6) is compared to equation (7) in figure 1 for the reference Mach number $M^* = q/a^*$. Figure 1 shows that throughout much of the transonic range the two relations agree well. Nevertheless, there are important differences. The possible expansion shock solution can no longer be excluded by the second law of thermodynamics as it is in the case of Rankine-Hugoniot flow. Also, through an isentropic shock wave, mass, energy, and entropy are conserved, but, transverse momentum is not conserved. For example, at $M_\infty = 1.4$, the one-dimensional momentum equation has the difference across the shock of

$$\left(\frac{p_2}{p_{st}} + \frac{\rho_2}{\rho_{st}} u_2{}^2\right) - \left(\frac{p_1}{p_{st}} + \frac{\rho_1}{\rho_{st}} u_1{}^2\right) = 0.0301 \tag{8}$$

Because momentum is not conserved across the shock, equation (1) contains a mechanism for drag production.

It is also a matter of interest to examine the shock relations for the transonic small perturbation equations. Consider, as a representative example, the small perturbation equation of Guderley, (ref. 4):

$$-\left(\frac{\gamma+1}{2}\right)^{3/2} \frac{\partial(u - \tilde{a}^*)^2}{\partial x} + \frac{\partial v}{\partial y} = 0 \tag{9a}$$

$$\frac{\partial u}{\partial y} - \frac{\partial v}{\partial x} = 0 \tag{9b}$$

where

$$\tilde{a}^* = \sqrt{\frac{2}{\gamma+1}}$$

Across a normal shock wave the jump relation for the Guderley equation is

$$(u_1 - \tilde{a}^*)^2 = (u_2 - \tilde{a}^*)^2 \tag{10}$$

Note that this relation, illustrated in figure 2 in terms of M^*, has a closed-form solution and closely approximates equation (6). The Guderley equation is not a valid approximation for subsonic, low-speed flow.

As a final example, consider the small perturbation equation of Spreiter (ref. 5)

$$\left[\left(1 - M_\infty{}^2\right) - (\gamma + 1)M_\infty{}^2\left(\frac{u}{q_\infty} - 1\right)\right] \frac{\partial u}{\partial x} + \frac{\partial v}{\partial y} = 0 \tag{11}$$

$$\frac{\partial u}{\partial y} - \frac{\partial v}{\partial x} = 0 \tag{12}$$

In this instance, the shock relation is a function of the free-stream Mach number and is given for a normal shock by

$$-\frac{2(1 + \gamma M_\infty{}^2)u_1}{(\gamma + 1)q_\infty M_\infty{}^2} + \left(\frac{u_1}{q_\infty}\right)^2 = \frac{-2\left(1 + \gamma M_\infty{}^2\right)u_2}{(\gamma + 1)q_\infty M_\infty{}^2} + \left(\frac{u_2}{q_\infty}\right)^2 \tag{13}$$

Figure 3 illustrates this relation for various choices of the free-stream Mach number. Clearly, this jump relation should not be used at lower free-stream Mach numbers if one intends to approximate Rankine-Hugoniot flow.

The transonic small disturbance equations conserve mass, momentum, and energy only to lowest order. Consequently, unlike Rankine-Hugoniot or isentropic flow, it is not clear that only a single mechanism produces wave drag. The normal shock relation for the Guderley equation (10) and the Spreiter equation (13) can also be obtained by an expansion of the Rankine-Hugoniot relations, and this approach is taken in references 4 and 5.

PROPER DIFFERENCING SCHEMES

The theory of a weak solution shows that the isentropic equations permit a possible discontinuity, which might be an expansion or a compression, and it is necessary that the numerical method be able to give these solutions. Here we are concerned with only the relaxation schemes and survey results, which demonstrate that proper difference schemes do in fact permit all possible solutions.

Murman and Cole (ref. 2) first demonstrated that shock waves can be established in the relaxation schemes if upwind (i.e., backwards) differencing formulas are used in the supersonic regions. This is the correct hyperbolic differencing scheme in the sense that it marches away from an initial data plane, and downstream influences cannot propagate upstream. Shock waves, when they form, appear where characteristics of the same family begin to coalesce in the supersonic flow. In a subsonic flow region, central difference schemes are used and these correctly bring in information from all directions — this is proper for elliptic equations.

Results obtained by using "proper differencing" are in good agreement with the jump predicted by the weak solution. The supersonic flow about a wedge as computed by relaxing the Guderley equations illustrates the capturing of the proper jump in figure 4. In this example, the equations were relaxed by the interchange algorithm of reference 6. In the more complex cases of transonic flow about airfoils, the numerical results predicted by proper mixed differencing are considered to agree well with experiment (see e.g., ref. 7). However, these solutions usually do not show a shock jump of the proper strength because a rapid expansion persists in the subsonic flow immediately behind the shock that is not resolved in a relatively coarse finite difference grid. A more detailed discussion of this flow phenomenon is given in reference 8.

The differencing schemes also permit multiple shocks to appear. An example of this flow is shown in figure 5, and again these results are plausible since similar results are found experimentally (see, e.g., ref. 9). The locations of these shocks have also been numerically tested and have been found to be fixed and independent of the path along which the solution was relaxed.

Numerical experiments with shock-free profiles show that the discontinuous solution is not spuriously forced into the flow field by the finite-difference procedure. Figure 6 illustrates the continuous surface pressure distribution about a thin "sine wave profile" in supersonic flow, which was found by means of the Guderley equations, and figure 7 illustrates the transonic flow found about a shock-free Nieuwland profile (ref. 10) using the method of reference 7. The very weak shocks that do appear in this latter solution are not attributed to the finite-difference procedure but to numerical truncation error and imperfection in describing the profile in the finite-difference network.

The theory of a weak solution also predicts the existence of an expansion shock, and yet this mathematically correct solution is never obtained when proper upwind differencing is used for supersonic flow regions. However, if downwind differencing is used in supersonic regions, the expansion shock will be found and the compression shock is excluded. Figure 8 illustrates this case as well as the conventional "physically correct" solution.[2] The important point to be made here is that the numerical method does have the capacity to give all of the allowable mathematical solutions, and solutions that do not model physics can be excluded.

A great deal of numerical experimentation was carried out to test the concept of proper differencing. A 6-percent-thick biconvex profile was used as a test case under conditions that give an embedded supersonic region terminated by a shock. With the proviso that the latter end of the supersonic region was terminated with proper upwind differencing, it was found that convergent and accurate iteration schemes could be devised that used central or other suitable interpolative differencing partly, and even substantially, into the supersonic region. However, the authors have never been able to devise a fully convergent iteration scheme when the differencing operators permitted disturbances to propagate both downstream and upstream throughout the entire supersonic region. Several of these schemes partially converged with almost shocklike shapes (see, e.g., ref. 6), and at least one scheme oscillated without diverging, but never did one of these schemes lead to a fully convergent solution.

---

[2] Similar expansion shock waves have been obtained with time-dependent schemes by computing in negative time. For optimum choice of the Courant number, the same type of downwind data is utilized.

PHYSICAL INTERPRETATION OF WAVE DRAG FROM ISENTROPIC SHOCK WAVES

In previous sections of this paper it has been shown that finite difference solutions of the isentropic flow relations can be arrived at that avoid physically incorrect behavior such as imbedded expansion shocks. At the same time, embedded compression shocks can be correctly accounted for. The question arises whether use of isentropic relations throughout a flow field including compression shocks can lead to a sufficiently accurate pressure distribution for evaluation of the wave drag. For example, Oswatitsch (ref. 11), has related the drag to entropy production in the flow field. If isentropic relations are used throughout an inviscid flow calculation including isentropic shocks, the entropy production is zero by definition. Nevertheless, it can be demonstrated that integration of the surface pressure calculated from the isentropic equations does lead to values of drag comparable to experimentally observed values if the shock Mach numbers are less than about 1.3. For example, figure 9 illustrates a comparison between experiment (refs. 12 and 13) and the results of drag calculations using surface pressure distributions calculated by the method of reference 7. The existence of a nonzero drag in spite of the contrary indication from the Oswatitsch drag relation can be attributed to the fact that momentum is not conserved across an isentropic shock. Proper interpretation of the Oswatitsch drag relation as applied to isentropic flows containing discontinuities leads to a basis for comparison of the drags computed for Rankine-Hugoniot and isentropic flows. The purpose of this and subsequent sections is to make such comparisons and to derive alternative methods for evaluation of the drag that are useful in conjunction with numerical solutions of the flow fields.

Oswatitsch has derived an approximate expression for the drag of an aerodynamic object in a steady flow in terms of the rate of entropy production

$$D = \frac{T_\infty}{q_\infty} \int_f \rho q_n (s - s_\infty) df \tag{14}$$

where T_∞, q_∞ are the temperature and velocity in the free stream. The integral is over a surface f that encloses all sources of entropy production in the flow field. The quantity q_n is the component of velocity in the direction of the outward normal to the surface of integration. According to von Karman (ref. 14), equation (14) is correct only to lowest order in $s - s_\infty$. For the steady inviscid flow considered here, shock waves are the only sources of entropy production. For a body in a subsonic or supersonic free stream, the integration can therefore be made over all shock waves according to the relation

$$D = \frac{T_\infty}{q_\infty} \sum \int_{\text{shock}} \rho_1 q_{n_1} \Delta s \, dA \tag{15}$$

where ρ_1 is the fluid density, q_{n_1} the normal component of velocity ahead of the shock, Δs the jump in entropy across the shock, and dA the element of shock surface area. The summation sign indicates that the results from integration over all shocks are to be added to obtain the total rate of entropy production in the flow field.

With proper interpretation, equation (15) applies to the weak solutions of the equations for irrotational, inviscid, adiabatic flow considered in this report. One method of arriving at a proper interpretation is to develop a physical model of the discontinuities so that such flows are included within the framework of those considered by Oswatitsch. The defining relations (eqs. (1) - (5)), are based on and are equivalent to conservation of mass, energy, and entropy in the entire flow field. It can be shown that the jump conditions for discontinuities (eqs. (4) and (5)) correspond to conservation of the component of momentum along the discontinuity but not the component of momentum normal to the discontinuity. Is there a physical model that corresponds to this anomaly? An inviscid flow can make a transition from supersonic to subsonic speed isentropically only by passing through a shock-free diffuser. Therefore, an isentropic normal shock is analogous to a surface covered by a large number of isentropic diffusers of vanishing extent in the streamwise direction (sketch (a)). The gain in momentum across the isentropic shock is balanced by the thrust on the diffusers. In the case of an oblique isentropic shock, the downstream ends of the diffusers are bent and contracted relative to the inlet ends (sketch (b)). The force on the diffusers is normal to the shock surface and the component of momentum tangent to the discontinuity is conserved.

With the foregoing interpretation of completely isentropic flow, including discontinuities, the Oswatitsch drag relation applies and shows that the total drag (body plus diffusers) is zero. Therefore, the drag on the body is equal to the thrust on the diffusers and the body drag is given by

$$D_i = \sum_{\text{shock}} \int \sin\theta \, \Delta\left(p + \rho q_n^2\right) dA \tag{16}$$

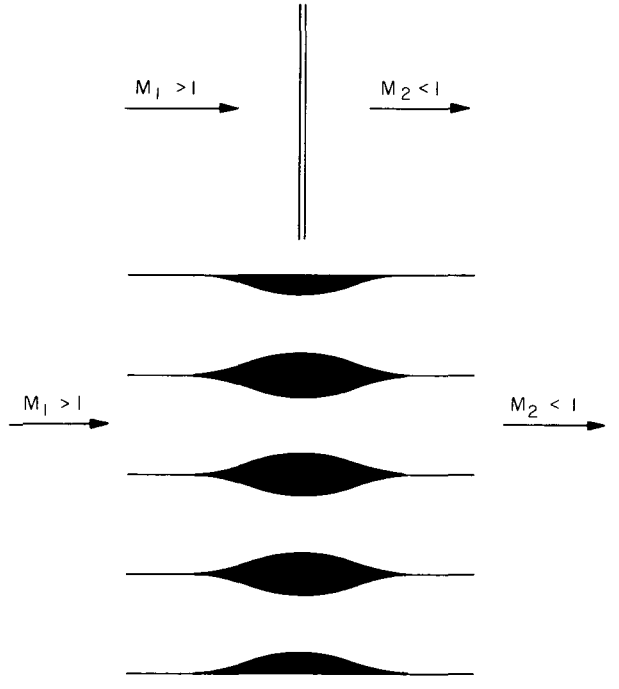

Sketch (a). - Isentropic normal shock.

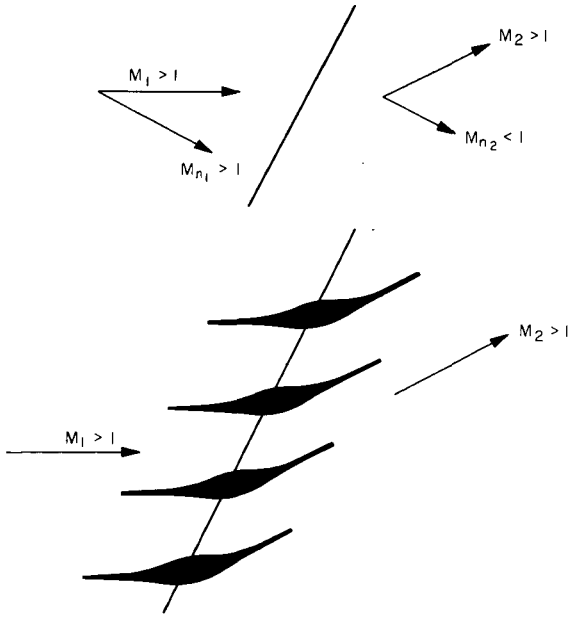

Sketch (b). - Isentropic oblique shock.

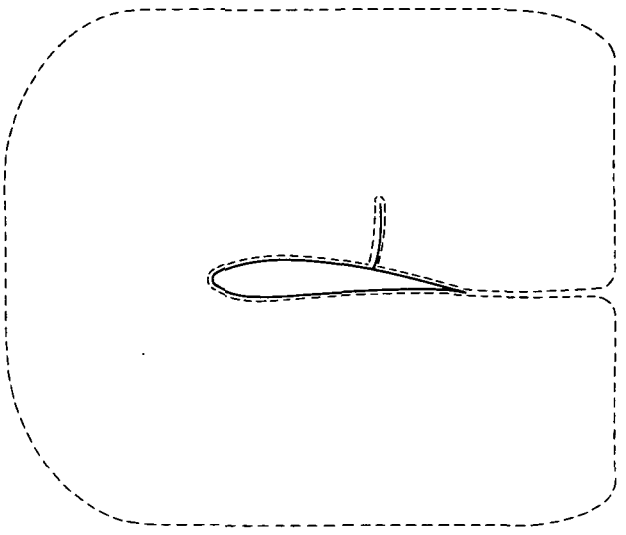

Sketch (c).

where θ is the angle of the shock relative to the free-stream direction and $\Delta(p + \rho q_n^2)$ is the increase in momentum normal to the shock. Again, the summation indicates that the contributions from all shocks are to be included.

A mathematical derivation of equation (16) that does not utilize a physical interpretation of isentropic shocks can also be indicated. It can be shown from the equations for continuous isentropic flow that the integral forms expressing the conservation of mass, momentum, and energy used by Oswatitsch apply for arbitrary closed contours that exclude discontinuities. Sketch (c) shows an example of an appropriate closed contour excluding a shock wave. The x momentum conservation relation applies on this contour.

$$\oint_f \left[p \cos(n,x) + \rho q_x q_n \right] df = 0$$

where n is the direction of the outward normal. For completely isentropic flow, conditions in the far flow field (including the wake) are the same as in the free stream so that the integral on the outer contour is zero. The integral over the body is equal to the drag. Evaluation of the integral over the isentropic shock then leads to equation (16).

COMPARISON OF DRAGS RESULTING FROM WEAK RANKINE-HUGONIOT AND ISENTROPIC SHOCK WAVES

It has been shown that weak isentropic shocks closely approximate Rankine-Hugoniot shocks so that the shock positions and upstream local Mach numbers can be assumed to be similar for the two types of flow over a given airfoil at the same free-stream Mach number. Consequently, the drag from an isentropic calculation can be compared with that from a calculation based on Rankine-Hugoniot shocks by comparing the integrands of equations (15) and (16) over a range of shock Mach numbers, thus avoiding the necessity for a complete knowledge of the flow field. For this purpose, equation (15) can be rearranged in the form

$$D = \frac{1}{M_\infty \sqrt{1 + \frac{\gamma - 1}{\gamma + 1}\left(M_\infty^2 - 1\right)}} \sum \int_{\text{shock}} \rho_1 q_{n1} a^* \frac{\Delta s}{\gamma R} dA \qquad (17)$$

where M_∞ is the free-stream Mach number and a^* is the speed of sound at a local Mach number of 1. For isentropic flow, equation (16) can be put in a similar form

$$D_i = \sum \int_{\text{shock}} \left[\sin\theta \frac{q_{n1}}{a^*} F\left(M_{n1}\right) \right] \rho_1 q_{n1} a^* \frac{(\Delta s)_{RH}}{\gamma R} dA \tag{18}$$

where

$$F\left(M_{n1}\right) = \frac{\gamma R \Delta \left(p + \rho q_{n1}{}^2\right)_i}{\rho_1 q_{n1}{}^2 (\Delta s)_{RH}} \tag{19}$$

The quantity $(\Delta s)_{RH}$ is the entropy jump across a Rankine-Hugoniot shock with upstream Mach number M_{n1} (based on the normal component of upstream velocity q_{n1}). The quantity $\Delta(p + pq^2{}_{n1})_i$ is the momentum increase normal to an isentropic shock with the same normal component Mach number M_{n1}. In equations (17), (18), and (19), ρ_1 is the fluid density immediately upstream of the shock and q_{n1} the normal component of upstream velocity.

From the jump conditions for a normal isentropic shock (eqs. (1c), (1d), and (6)), the Rankine-Hugoniot normal shock relations, and the equations of state (e.g., ref. 15), it can be shown that both numerator and denominator of equation (19) are of order $(M_{n1} - 1)^3$ for weak shocks. The quantity $F(M_{n1})$ is equal to 1.0 to lowest order in $(M_{n1} - 1)$ and deviates from 1.0 by less than 15 percent for $M_{n1} < 1.4$. For a supersonic free stream with weak oblique shocks, the factor in square brackets in equation (18) is

$$\sin\theta \frac{q_{n1}}{a^*}\left(F M_{n1}\right) \simeq \frac{1}{M_\infty \sqrt{1 + \frac{\gamma - 1}{\gamma + 1}\left(M_\infty{}^2 - 1\right)}} + O\left(M_{n1} - 1\right) \tag{20a}$$

Thus to lowest order in $(M_{n1} - 1)$ the drag for supersonic isentropic flow with oblique shocks (eq. (18)) is identical to that for supersonic flow with Rankine-Hugoniot shocks (eq. (17)). However, for a subsonic free stream with weak normal shocks, the isentropic flow solution yields a drag that differs from that for the corresponding flow with Rankine-Hugoniot shocks. In this case

$$\sin\theta \frac{q_{n1}}{a^*} F\left(M_{n1}\right) \simeq 1.0 + O\left(M_{n1} - 1\right) \tag{20b}$$

and to lowest order in $(M_{n1} - 1)$ does not match the factor outside the integral in equation (17). Table 1 summarizes the factors entering the expression for the isentropic drag and indicates a correction factor D/D_i for supersonic and subsonic flow.

TABLE 1 - FACTORS IN EXPRESSION FOR DRAG IN ISENTROPIC FLOW (EQ. (18))

Flow Mach number	$\sin\theta$	$\frac{q_{n1}}{a^*}$	Correction factor D/D_i
Supersonic free stream $(M_\infty > 1.0)$			
weak oblique shock	$\approx\frac{1}{M_\infty}$	$\approx \frac{1}{\sqrt{1+\frac{\gamma-1}{\gamma+1}\left(M_\infty{}^2-1\right)}}$	1.0
Subsonic free stream $(M_\infty < 1.0)$			
weak normal shock	≈ 1.0	≈ 1.0	$\frac{1}{M_\infty\sqrt{1+\frac{\gamma-1}{\gamma+1}\left(M_\infty{}^2-1\right)}}$

The assumptions used in the derivation of the correction factors listed in table 1 may be summarized as follows:

1. Inviscid adiabatic flow of a perfect gas.
2. Exact isentropic flow relations apply along streamlines in regions where there are no discontinuities.
3. Terms of order $(s - s_\infty)^2$ and higher are negligible in Rankine-Hugoniot flow.
4. Terms of order $(M_{n1} - 1)^4$ and higher are negligible in the evaluation of entropy increase through Rankine-Hugoniot shocks.
5. Terms of order $(M_{n1} - 1)^4$ and higher are negligible in the evaluation of momentum increase through isentropic shocks.
6. The location and upstream local Mach number of shocks is the same for Rankine-Hugoniot and isentropic flow.
7. Oblique shocks are at angle $\sin^{-1}\left(M_\infty{}^{-1}\right)$ and normal shocks perpendicular to the free-stream direction.

The limits of validity of these assumptions will be discussed later.

Previous approximate treatments of transonic flow are typically based on a different set of assumptions. For example, in ref. 16 an expansion procedure is described that is based on the limit process ($\delta \to 0$, $M_\infty \to 1$; $k = (1 - M_\infty^2)/\delta^{2/3}$ and $\delta^{1/3}y$ fixed) where δ is the thickness to chord ratio. The assumptions for table 1 are less restrictive than the lowest order equations from the expansion in δ of reference 16, but are equivalent to them at $M_\infty = 1$. Thus both apporaches lead to the prediction that the correction factor D/D_i is equal to 1.0 at $M_\infty = 1.0$ to lowest order in δ (and hence lowest order in $(M_{n1} - 1)$ for shocks). However, the results in table 1 are not restricted to

$M_\infty \to 1$ so long as the shocks are weak and hence apply to thick airfoils near the point of drag rise. If the drag rise Mach number is as low as 0.7, the correction factor indicated in table 1 becomes 40 percent.

The magnitude of the correction is illustrated in figure 9 where it is applied to isentropic calculations and the results compared to wind-tunnel data. In these cases the assumption that $F(M_{n1})(q_{n1}/a^*) \to 1.0$ breaks down quite rapidly with increasing shock strength as will be shown later.

It is of interest to consider the efficacy of applying the foregoing correction factors when the shocks are not weak. For that purpose several approximations used in the foregoing derivations have been examined in more detail. The Oswatitsch drag relation (eq. (14)) is itself an approximation that depends on the assumption that the velocity and thermodynamic state in the far wake do not differ appreciably from free-stream conditions. This fact may not be significant unless the relation is to be used for quantitative rather than qualitative evaluation of the drag. Since the relation will be used for that purpose in this report, the magnitude of error introduced by the Qswatitsch approximation is of particular interest. An exact relation for inviscid flow over airfoils has been derived, corresponding to the Oswatitsch drag relation, which is found to be in error by no more than 4 percent in the range of interest (free-stream Mach numbers between 0.7 and 2.0 and shock Mach numbers up to 1.4). The derivation is given in appendix A.

In the derivation of correction factors listed in table 1, use was made of assumption (6) that the shock position and shock Mach number M_{n1} were approximately the same for isentropic flow and flow with Rankine-Hugoniot shocks. It is difficult to assess the validity of this assumption in the case of strong shocks without obtaining the two solutions. When the free stream is supersonic exact solutions for flow over wedges are available for such a comparison. It is shown in appendix B that the correction factor of 1.0 for oblique shocks in a supersonic stream given in table 1 is valid for shock Mach numbers less than 1.4, even though the shock Mach number M_{n1} is not the same for Rankine-Hugoniot and isentropic flows. This result is due to the compensating effect of higher order terms in equation (20a). It has not been shown that the same compensating effect is valid for the subsonic case. Further details of the effects of shock strength are given in appendix B.

SHOCK INTEGRATION METHOD FOR EVALUATING WAVE DRAG

It is difficult to evaluate the wave drag accurately by integrating the pressure distribution on a body when the pressure is determined from a finite-difference solution. This difficulty arises because the drag is equal to a small difference between pressure forces on forward-facing and rearward-facing surface elements and there is difficulty in specifying the body shape with sufficient accuracy in a finite-difference grid. The calculations of figure 9, for example, showed a small "tare" drag – a slight thrust at subcritical speed – which had to be subtracted from the results. In contrast, the evaluation of lift and moment is less sensitive to small errors in a finite-difference solution because these quantities do not involve small differences.

The previously developed relationships between drag and shock jump conditions offer a method for accurately obtaining wave drag that is not as sensitive to the body geometry or small numerical

errors. In this section, specific formulas for that purpose are presented that are based on flow conditions before the shock. Thus, the effect of the expansion singularity that can exist behind a normal shock in transonic flow (noted earlier) is excluded from these formulas. The required formulas are summarized below and detailed information on the derivations is given in appendix C. Results from sample calculations using this approach will be given later.

For isentropic flow the drag coefficient of an airfoil can be evaluated by means of equation (16) as follows

$$C_D = \frac{2}{c} \sum \int_{\text{shock}} \Delta P \frac{\rho_1}{\rho_\infty} \left(\frac{q_{n1}}{q_\infty}\right)^2 \sin\theta \, dz \tag{21}$$

where z is the distance along the shock. To evaluate the integrand (for $\gamma = 1.4$) the following quantities must be computed at each point on the shock surface. The relation

$$r + r^2 + r^3 + r^4 + r^5 = \frac{1 - \frac{1}{5}\left(u_1^2 + v_1^2\right)}{u_1^2 (\sin\theta - \cos\theta \, v_1/u_1)^2} \tag{22}$$

is solved for r in the interval $0 < r < 1$. (Any conventional technique for finding roots can be used to evaluate r since the left side of equation (22) is monotonic in the interval from 0 to 1). The quantities ΔP, ρ_1/ρ_∞, q_{n1}/q_∞ can then be evaluated (for $\gamma = 1.4$) from the relations

$$\Delta P = \frac{1}{5}\left(1 - r^{5/2}\right) \left[\frac{\left(1 + r^{5/2}\right)\left(1 + r + r^2 + r^3 + r^4 + r^5 + r^6\right)}{\left(1 + r^{7/2}\right) r^{5/2}} - 7\right] \tag{23}$$

$$\frac{\rho_1}{\rho_\infty} = \left[\frac{1 - \frac{1}{5}\left(u_1^2 + v_1^2\right)}{1 - \frac{1}{5} u_\infty^2}\right]^{5/2} \tag{24}$$

$$\frac{q_{n1}}{q_\infty} = \frac{u_1}{u_\infty}\left[\sin\theta - \cos\theta \left(v_1/u_1\right)\right] \tag{25}$$

where θ is the angle of the shock with respect to the x axis. If $80° < \theta < 100°$, the factor $\cos\ \theta\ (v_1/u_1)$ is negligible. Also if errors in drag of the order of 5 percent are tolerable, $\sin\theta$ can be set equal to 1.0 and $v_1{}^2$ neglected compared to $u_1{}^2$ in the above relations when the free stream is subsonic.

For flow with Rankine-Hugoniot shocks, the drag coefficient of an airfoil can be evaluated according to equation (A4) as follows

$$C_D = \frac{2}{c} \sum \int_{\text{shock}} \Delta G \frac{\rho_1}{\rho_\infty} \frac{q_{n1}}{q_\infty} dz \tag{26}$$

At each point on the shock surface the following quantities are to be computed ($\gamma = 1.4$)

$$M_{n1} = \frac{u_1 \left[\sin\theta - \cos\theta \left(v_1/u_1\right)\right]}{\sqrt{1 - \frac{1}{5}\left(u_1{}^2 + v_1{}^2\right)}} \tag{27}$$

$$\frac{\Delta s}{R} = \frac{7}{2} \ln\left(\frac{5}{6M^2{}_{n1}} + \frac{1}{6}\right) + \frac{5}{2} \ln\left(\frac{7}{6}\ M^2{}_{n1} - \frac{1}{6}\right) \quad \text{(ref. 15)} \tag{28}$$

$$\Delta G = \sqrt{1 + \left(1 - \frac{5}{u_\infty{}^2}\right)\left(1 - e^{\frac{2}{7}\frac{\Delta s_1}{R}}\right)} - \sqrt{1 + \left(1 - \frac{5}{u_\infty{}^2}\right)\left(1 - e^{\frac{2}{7}\frac{\Delta s_1}{R}}\ e^{\frac{2}{7}\frac{\Delta s}{R}}\right)} \tag{29}$$

where $\Delta s_1 = s_1 - s_\infty$ is the deviation of the specific entropy ahead of the shock from the free-stream value. If only one shock wave is present or if errors in drag less than.4 percent are tolerable, Δs_1 can be set equal to zero. Furthermore, expansion of equation (29) to order $\Delta s/R$ and $\Delta s_1/R$ leads to the Oswatitsch approximation

$$\Delta G \simeq \frac{1}{7}\left(\frac{5}{u_\infty{}^2} - 1\right)\frac{\Delta s}{R}$$

which also leads to evaluation of drag accurate to within 4 percent for values of $M_{n1} < 1.4$ (see appendix A). The quantities ρ_1/ρ_∞ and q_{n1}/q_∞ are given in equations (24) and (25).

If a finite-difference solution of the flow equations with Rankine-Hugoniot shocks is available, equations (26) through (29) are appropriate for evaluation of the drag coefficient. If finite-difference solutions with isentropic shocks are of interest, equations (21) to (25) provide an accurate value of C_D corresponding to integration of pressure forces on the body. However, the drag coefficient from equations (26) through (29) is also of interest for isentropic flow solutions, since it corresponds to a "corrected" value under the assumption that the position and Mach number based on the normal component of velocity ahead of the isentropic shock are approximately the same as for a Rankine-Hugoniot shock. With a subsonic freestream this assumption is valid near the point of drag rise where the shock is not strong, but its validity has not been established for cases in which the shock strength is appreciable. The difference between the two drag coefficients is perhaps indicative of the possible error in either value when the shocks are strong.

NUMERICAL EVALUATIONS OF WAVE DRAG

The wave drag formulas, equations (21) and (26), have been incorporated in a relaxation routine developed for equations (1) and (9). The program was written for thin airfoil boundary conditions and in these tests employed a uniform, finite-difference grid with a relatively coarse spacing (20 points along the chord). For these reasons, the usual means of evaluating drag by a pressure integration is not very satisfactory.

Computational results for wave drag based on conditions ahead of the shock wave are illustrated in figure 10 for flow over a biconvex profile. The experimental data of Knechtel (ref. 17), at a Reynolds number of about 2 million, are also shown for comparison. The numerical calculations are actually based on equation (9), but the shock relations as shown by figure 2 are essentially identical to those of equation (1). The data were used in evaluating both equation (21) and (26) as shown in figure 10, and although the difference in wave drag is increasing as M_∞ increases, the percentage difference diminishes. This trend is predicted by the correction factor listed in table 1, even though the calculations indicate that the assumption $q_{n_1} \simeq a^*$ is violated on this airfoil as M_∞ increases.

The agreement between the inviscid calculation and the experiment is considered to be reasonably good even though a coarse mesh is used. Furthermore, shock induced separation of a fully developed turbulent boundary layer is not expected to occur until $M_n \simeq 1.30$ to 1.4 (refs. 18 and 19)[3], and the numerical calculations indicate that $M_n = 1.35$ is not reached until $M_\infty \to O(0.93)$. In the absence of boundary-layer separation, the inviscid calculations correspond to infinite Reynolds number and are likely to be a better approximation to full-scale flight conditions than the low Reynolds number data of the wind tunnel.

An essential point is that the wave drag is evaluated independently of the pressure distribution at the nose of the profile. Therefore, if a method employing thin airfoil assumptions can accurately predict the strength and location of a shock, wave drag can be accurately evaluated. The drag calculations based on either equation (21) or (26) is also independent of how well the method captures the expansion singularity that trails the normal shock in transonic flow. Indeed,

[3] It is fortuitous that for transonic flow over airfoils the inviscid and isentropic assumptions (see fig. 1) break down almost simultaneously.

this method of computing wave drag is insensitive to any overshoots or oscillations behind a shock and the small precursor waves common to many shock capturing (e.g., ref. 20) schemes should not present a very formidable problem.

Any drag calculation is sensitive to the location of the shock wave, and the shock location itself is very sensitive to numerical truncation errors that accompany any finite-difference procedure. Because the drag rise is sharp, a numerical procedure employing a relatively coarse grid may yield a result with substantial error. However, the Mach number at which a given drag is reached should be predicted within ±0.01 or ±0.02. Reliable, high Reynolds number transonic experiments are now required, which can be used to calibrate the numerical calculations.

CONCLUDING REMARKS

In this paper an attempt was made to assess the assumption of isentropic flow in the numerical calculation of transonic flow. Study of the properties of weak solutions shows that the compressible irrotational flow equations do admit shock waves through which momentum is not conserved. Results from a series of numerical experiments also demonstrated that relaxation procedures that use proper differencing do give the correct mathematical behavior and that incorrect physical behavior such as embedded expansion shocks can be avoided.

With this established background, a detailed analysis of the drag mechanism in isentropic flow was presented. It was shown in this study that a correction factor is appropriate if the drag is to be evaluated from a solution that includes isentropic shock waves. The method of evaluation that was developed for the wave drag is relatively insensitive to the use of approximations such as thin airfoil boundary conditions when the shock location and strength are adequately predicted. Examples of the use of this technique were presented and the results compared with experiments.

It is conjectured that in the absence of strong viscous effects, current finite-difference solutions which utilize transonic approximations, supplemented by methods developed in this paper, are adequate for prediction of the wave drag near the point of drag rise or for predicting the Mach number at which a given level of wave drag will occur.

Ames Research Center
National Aeronautics and Space Administration
Moffett Field, Calif. 94035, July 10, 1972

APPENDIX A

EXACT RELATION BETWEEN ENTROPY PRODUCTION AND WAVE DRAG IN INVISCID FLOW

The drag relation of Oswatitsch (Eq. (14)), is based on the approximation that the velocity and thermodynamic state in the wake do not differ appreciably from free-stream conditions. It is of interest to determine the corresponding exact relation for inviscid flow. An exact relation contained in the derivation of Oswatitsch can be written

$$D = q_\infty \oint_{f_\infty} \rho q_n \left(1 - \frac{q_x}{q_\infty}\right) df \tag{A1}$$

where q_x is the component of velocity in the free-stream direction, and the surface of integration f_∞ is sufficiently far from the object on which the drag is exerted that at f_∞ the deviation of the pressure from the free-stream pressure is negligible. The only contribution to this integral is in the wake. Therefore, q_x can be evaluated by considering the flow along streamlines from $-\infty$ to the wake region. For inviscid flow, the total enthalpy, $h_{st} = h + (1/2)q^2$, is conserved

$$h_{st} = h_{st_\infty}$$

and the total pressure, $p_{st} = p + (1/2)\rho q^2$, depends on the entropy increase according to the relation

$$p_{st} = p_{st_\infty} e^{-(s-s_\infty)/R}$$

and

$$p = p_\infty \quad \text{(in the far wake)}$$

Combining these relations with the equations of state for a perfect gas and rearranging them according to relations given in reference 15 leads to an expression for q_x/q_∞ in terms of M_∞ and $s - s_\infty$. Substitution of that expression into equation (A1) yields

$$D = q_\infty \oint_{f_\infty} \rho q_n G\left(M_\infty, s - s_\infty\right) df \tag{A2}$$

where

$$G\left(M_\infty, s - s_\infty\right) = 1 - \sqrt{1 + \frac{2}{(\gamma - 1)M_\infty^2}\left[1 - e^{\left(\frac{\gamma - 1}{\gamma}\right)\left(\frac{s - s_\infty}{R}\right)}\right]} \tag{A3}$$

Equations (A2) and (A3) can also be derived from a relation given by Lighthill (ref. 21). The integrand in equation (A2) is equal to the integrand of equation (A1) on the surface of integration f_∞ far from the body, but not elsewhere. Other surfaces of integration can be considered for evaluation of equation (A2) if it can be shown that the same value of the integral will be obtained. Since G is a function only of M_∞ and $s - s_\infty$, within a region where entropy changes do not occur, G is constant along streamlines. Therefore, G can be taken outside the integral for surfaces that enclose segments of stream tubes of infinitesimal cross-sectional area. The integral over such surfaces of the remaining integrand ρq_n is zero. Consequently, f_∞ may be moved across regions in which entropy is constant without affecting the value of the integral in equation (A2). The surface f_∞ may therefore be replaced by any surface f that encloses all changes of entropy (and hence changes of G). For the steady inviscid flow considered here, shock waves are the only source of entropy changes. Therefore equation (A2) can be replaced by

$$D = q_\infty \sum_{\text{shock}} \int \rho_1 q_{n1} \Delta G \, dA \tag{A4}$$

As in equation (15), the subscript 1 denotes conditions immediately upstream of the shock, q_{n1} is the upstream component of velocity normal to the element of shock area dA and ΔG is the jump in G across the shock corresponding to the jump in $s - s_\infty$ according to equation (A3). The summation sign indicates that results from integration over all shocks are to be added. Expansion of equation (A3) to lowest order in $s - s_\infty$, substitution in equation (A4) and rearrangement lead to equation (15), which was derived from the approximate Oswatitsch drag relation. It should be noted that there are restrictions on the applicability of the exact relationship between drag and entropy increase derived here. In addition to the assumptions of inviscid adiabatic flow, the pressure in the far wake was taken to be equal to the free-stream pressure and the direction of flow in the far wake was taken to be that of the free stream. The presence of trailing vortices in three-dimensional flow would require a separate treatment.

Figure 11 shows the fractional error of the Oswatitsch drag relation corresponding to the lowest order approximation $O(\Delta s/R)$ of the jump in G across a shock wave. The fractional error is plotted versus the shock Mach number based on the component of velocity normal to the shock with free-stream Mach numbers of 0.7, 1.0, and 2.0. For shock Mach numbers M_{n1} less than 1.4 the error is less than 4 percent if the free stream Mach number is greater than 0.7.

APPENDIX B

ASSUMPTIONS USED TO DETERMINE THE DRAG CORRECTION FACTORS OF TABLE 1

In the derivation of the correction factors listed in table 1 it was assumed that the shock position and shock Mach number M_{n1} are approximately the same for isentropic flows and flows with Rankine-Hugoniot shocks if the shocks are weak. It is of interest to examine these assumptions when the shocks are not weak. Figure 12 shows the variation of the function $F(M_{n1})$ and the product $(q_{n1}/a^*)\ F(M_{n1})$ versus M_{n1}. The deviation of the latter quantity from 1.0 suggests that for strong shocks, a correction factor considerably different from that indicated in table 1 may be appropriate for subsonic flows. For supersonic flow with oblique shocks $\sin\theta$ and q_{n1}/a^* depend on M_∞ as well as M_{n1}. Figure 13 shows the variation of $\sin\theta\ (q_{n1}/a^*)\ F(M_{n1})$ (isentropic flows) versus M_∞ with M_{n1} as parameter. For comparison, the factor

$$F_\infty = 1/M_\infty \sqrt{1 + \frac{\gamma - 1}{\gamma + 1}\left(M_\infty^{\,2} - 1\right)}$$

contained in equation (17) is also shown in Figure 13 as a solid curve. For weak shocks ($M_{n1} < 1.01$) the factor inside the integral of equation (18) closely approximates the factor outside the integral in equation (17). For stronger shocks, however, the deviation is appreciable.

It is difficult to assess the validity of assumption (6) (listed after table 1) in the case of strong shocks with subsonic free stream in the absence of data for both cases. When the free stream is supersonic, however, exact solutions for flow over wedges provide the necessary information. A suitable configuration is one incorporating forward facing and rearward facing wedges separated by an extended region of constant thickness as shown in sketch (d).

It is useful to consider separately cases in which the entropy production is confined to either the forward shock or the rear shock by letting either δ_f or δ_r approach zero while holding t fixed. Since the extent of the shock tends toward infinity, it might be questioned whether the resulting entropy production can be neglected as δ approaches zero. However, this question is answered by the following observation. If we let both δ_f and δ_r approach zero, the total drag (and hence the total entropy production) will approach zero. Further, if we let δ_f alone approach zero, the pressure p_f will approach p_∞, and the flow immediately ahead of the rearward-facing wedge can be taken to be the same as that in the free stream. In that case the drag coefficient (based on a chord length $t/\sin\delta_r$) is

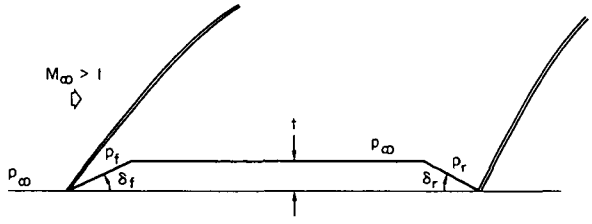

Sketch (d).

$$C_D = \frac{2}{\gamma M_\infty{}^2}\left(1 - \frac{p_r}{p_\infty}\right)\sin \delta_r \quad (\delta_f \to 0)$$

With $\delta_f \to 0$, the pressure p_r on the rearward-facing wedge is determined by the Prandtl-Meyer expansion through the turning angle δ_r starting from free-stream conditions. This remains true whether the rear shock is isentropic or a Rankine–Hugoniot shock. Consequently it is clear that the drag is the same regardless of whether isentropic or Rankine-Hugoniot shocks are used as long as δ_r is less than the value at which the shock at the end of the body becomes curved. According to equation (A4) the drag is related to the entropy production in the rear shock, entropy production being negligible in the front shock. Or with isentropic shocks the drag is related to the momentum defect across the rear shock according to equation (16). Since the drags are equal for the two types of flow, it follows that the shock Mach number based on the velocity component normal to the shock must be different for an isentropic than for a Rankine-Hugoniot shock. Without making calculations we find that in this case the isentropic drag correction factor of 1.0 for weak oblique shocks in table 1 remains valid for a wide range of shock strengths even though the assumption of equal shock Mach numbers used in the construction of figure 13 is not valid.

As another example, consider the case in which δ_r approaches zero so that the strength of the rear shock is negligible and the pressure on the rearward-facing wedge deviates from the free-stream pressure by a negligible amount. Then the drag coefficient based on a chord length $t/\sin \delta_f$ is

$$C_D = \frac{2}{\gamma M_\infty{}^2}\left(\frac{p_f}{p_\infty} - 1\right)\sin \delta_f \quad (\delta_r \to 0)$$

In this case p_f and the drag do depend on whether isentropic or Rankine–Hugoniot shock relations are used. It is necessary to evaluate the two drags to make a comparison. This has been done using the relations for flow over a wedge given in reference 22 and the corresponding relations for wedge flow with isentropic shocks given in appendix C. Figure 14 shows C_D versus δ_f for the two types of flow at free–stream Mach numbers $M_\infty = 1.4$ and 2.0. At $M_\infty = 1.4$, the two drags are quite close until the critical wedge angle (at about 9.5°) is approached. The unfaired points correspond to the strong family of oblique shocks for which the shock would be curved near the wedge and the drag coefficient is not given correctly by the above formula. The Mach number based on the component of velocity normal to the shock, M_{n1}, is indicated at individual points for comparison. At $M_\infty = 2.0$, the deviation between the two drags is imperceptable in this plot even when the shock Mach number based on the normal component of velocity is as large as 1.4. These results show that the difference in Rankine–Hugoniot and isentropic shock strengths is not always enough to make the two drags equal. Nevertheless, for the cases considered, the weak shock correction factors of table 1 are more nearly valid than the correction factors arrived at by retaining for strong shocks the assumption that the isentropic shock Mach number is the same as the Rankine–Hugoniot shock Mach number for the same airfoil. There is no assurance that this is true for cases in which the free-stream velocity is subsonic.

APPENDIX C

DERIVATION OF JUMP CONDITIONS ACROSS ISENTROPIC SHOCK

An isentropic normal shock is defined by the isentropic channel flow relations (e.g., ref. 15) plus the requirement that the stream tube area of the subsonic state be equal to that of the supersonic state. From equation (4.19) of reference 15 this requirement is expressed by the relation

$$\frac{M_2^2}{M_1^2} = \left(\frac{1 + \frac{\gamma - 1}{2} M_2^2}{1 + \frac{\gamma - 1}{2} M_1^2} \right)^{\frac{\gamma+1}{\gamma-1}} \tag{C1}$$

where M_1 and M_2 are the Mach numbers ahead of and behind the shock. Replacing M_2^2 on the right with $M_1^2 (M_2^2/M_1^2)$ and solving for M_1^2 yields

$$M_1^2 = \frac{2}{\gamma - 1} \left[\frac{1 - r}{r - r^{\left(\frac{\gamma+1}{\gamma-1}\right)}} \right] \tag{C2}$$

where

$$r = \left(\frac{M_2^2}{M_1^2} \right)^{\frac{\gamma-1}{\gamma+1}} \tag{C3}$$

Also, from equations (C1) and (C3)

$$\frac{1 + \frac{\gamma - 1}{2} M_2^2}{1 + \frac{\gamma - 1}{2} M_1^2} = r \tag{C4}$$

The pressure ratio across the shock can be found from equation (4.14b) of reference 15 and is

$$\frac{p_2}{p_2} = \left(\frac{1 + \frac{\gamma - 1}{2} M_1^2}{1 + \frac{\gamma - 1}{2} M_2^2} \right)^{\frac{\gamma}{\gamma - 1}}$$

or upon substitution of equation (C4),

$$\frac{p_2}{p_1} = r^{\left(\frac{\gamma}{\gamma - 1}\right)} \tag{C5}$$

Since $\rho_2 \; q_2 = \rho_1 q_1$, the velocity ratio can be evaluated from the relation for density variations in isentropic flow (equation (4.14c), ref. 15) and we obtain

$$\frac{q_2}{q_1} = \frac{\rho_1}{\rho_2} = r^{\frac{1}{\gamma - 1}} \tag{C6}$$

The pressure and velocity ratios could be expressed in terms of the Mach number ahead of the shock, M_1 if equation (C2) could be solved for r in terms of M_1. This is not possible without resorting to numerical techniques. The numerical inversion can be made less troublesome if the reciprocal of equation (C2) and the identity

$$\frac{1 - r^n}{1 - r} = 1 + r + r^2 + \ldots r^{n-1} \quad (n \text{ integer}) \tag{C7}$$

are used to obtain

$$r + r^2 + r^3 + \ldots r^{\frac{2}{\gamma - 1}} = \frac{2}{(\gamma - 1) M_1^2} \tag{C8}$$

With $\gamma = 7/5$, the polynomial on the left is $r + r^2 + r^3 + r^4 + r^5$. The root of interest lies in the interval

$$\left(\frac{1}{M_1^2} \right)^{\frac{2}{\gamma - 1}} < r < \frac{1}{M_1^2}$$

There is only one real root in this interval since all the terms on the left are positive and increase monotonically with increasing r.

Once the quantity r is determined, the momentum loss across the shock can be evaluated in terms of r with the aid of the foregoing relations. From isentropic flow relations in reference 15, we have

$$\Delta\left(p+\rho q^2\right) = \left(\rho_1 q_1{}^2\right)\left[\frac{1}{\gamma M_1{}^2}\left(\frac{p_2}{p_1}-1\right)+\frac{q_2}{q_1}-1\right]$$

Substituting equations (C2), (C5), (C6), and (C7) and rearranging leads to the expression

$$\Delta\left(p+\rho q^2\right) = \frac{\gamma-1}{2}\rho_1 q_1{}^2\left(1-r^{\frac{1}{\gamma-1}}\right)\left[\frac{\left(1+r^{\frac{1}{\gamma-1}}\right)\left(1+r+r^2+\ldots r^{\frac{\gamma-1}{\gamma+1}}\right)}{\left(1+r^{\frac{2\gamma}{\gamma-1}}\right)\left(r^{\frac{1}{\gamma-1}}\right)}-\frac{2\gamma}{\gamma-1}\right] \tag{C9}$$

The foregoing normal shock relations apply also to oblique shocks upon replacement of q_1 by the normal component of velocity q_{n1} and replacement of M_1 by M_{n1}, the Mach number corresponding to q_{n1}. Then for the general case (oblique or normal shocks)

$$r+r^2+r^3+\ldots r^{\frac{2}{\gamma-1}} = \frac{2}{(\gamma-1)M_{n1}^2} \tag{C10}$$

$$\Delta\left(p+\rho q^2\right) = \Delta P\frac{\rho_1}{\rho_\infty}\left(\frac{q_{n1}}{q_\infty}\right)^2 \tag{C11}$$

$$\Delta P = \left(1-r^{\frac{1}{\gamma-1}}\right)\left[\frac{\left(1+r^{\frac{1}{\gamma-1}}\right)\left(1+r+r^2+\ldots r^{\frac{\gamma-1}{\gamma+1}}\right)}{\left(1+r^{\frac{2\gamma}{\gamma-1}}\right)r^{\frac{1}{\gamma-1}}}-\frac{2\gamma}{\gamma-1}\right] \tag{C12}$$

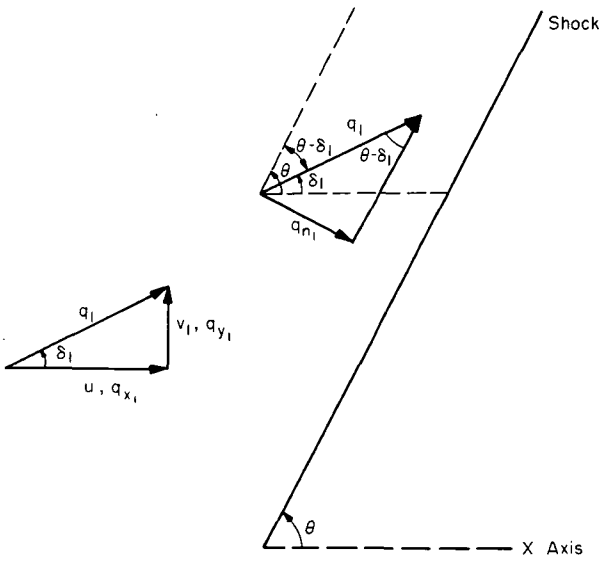

Sketch (e). - Velocity components ahead of shock.

If the flow ahead of the shock is at an angle δ_1 with respect to the x axis (i.e., $q_{x1} = q_1 \cos \delta_1$), and the shock is at an angle θ with respect to the x axis, it can be seen from sketch (e) that

$$\frac{q_{n1}}{q_\infty} = \frac{q_{x1}}{q_\infty} \frac{\sin(\theta - \delta_1)}{\cos \delta_1}$$

or in terms of the dimensionless velocities $u_1 = q_{x1}/a_{st}$, $v_1 = q_{y1}/a_{st}$,

$$\frac{q_{n1}}{q_\infty} = \frac{u_1}{u_\infty} \left[\sin \theta - \cos \theta \left(v_1/u_1\right)\right] \quad \text{(C13)}$$

With the aid of the relationship

$$1 + \frac{\gamma - 1}{2} M_1^2 = \left[1 - \frac{\gamma - 1}{2} \left(u_1^2 + v_1^2\right)\right]^{-1}$$

the density ratio ρ_1/ρ_∞ can be expressed as

$$\frac{\rho_1}{\rho_\infty} = \left[\frac{1 - \frac{\gamma - 1}{2} \left(u_1^2 + v_1^2\right)}{1 - \frac{\gamma - 1}{2} u_\infty^2}\right]^{\frac{1}{\gamma - 1}} \quad \text{(C14)}$$

Also the shock Mach number based on the component of velocity normal to the shock is related to the dimensionless velocities by

$$M_{n1} = \frac{u_1 \left[\sin \theta - \cos \theta \left(v_1/u_1\right)\right]}{\sqrt{1 - \frac{\gamma - 1}{2} \left(u_1^2 + v_1^2\right)}} \quad \text{(C15)}$$

REFERENCES

1. Lax, Peter D.: Weak Solutions of Nonlinear Hyperbolic Equations and Their Numerical Computation. Communs. Pure Appl. Math., vol. VII, no 1. Feb. 1954, pp. 159-193.

2. Murman, Earll M.; and Cole, Julian D.: Calculation of Plane Steady Transonic Flows. AIAA J., vol. 9, no. 1. Jan. 1971, pp. 114-121.

3. Lomax, Harvard; Kutler, Paul; and Fuller, Franklyn B.: The Numerical Solution of Partial Differential Equations Governing Convection. AGARDograph-146-70, Oct. 1970.

4. Guderley, K. G.: The Theory of Transonic Flow. Pergamon Press, N.Y. 1962.

5. Spreiter, John R.: On the Application of Transonic Similarity Rules to Wings of Finite Span. NACA Rep. 1153, 1953.

6. Steger, Joseph L.; and Lomax, Harvard: Generalized Relaxation Methods Applied to Problems in Transonic Flow. Second International Conference on Numerical Methods in Fluid Dynamics. Lecture Notes in Physics, vol. 8, Springer-Verlag, N.Y., 1971, pp. 193-198.

7. Steger, J. L.; and Lomax, H.: Numerical Calculation of Transonic Flow About Two-Dimensional Airfoils by Relaxation Procedures. AIAA Paper 71-569, 1971.

8. Emmons, Howard W.: Flow of a Compressible Fluid Past a Symmetrical Airfoil in a Wind Tunnel and in Free Air. NACA TN 1746, 1948.

9. Kacprzynski, J. J., Ohman, L. H., Garabedian, P. R., Korn, D. G.: Analysis of the Flow Past a Shockless Lifting Airfoil in Design and Off-Design Conditions. Natl. Res. Council of Canada, Ottawa Rep. LR-554, 1971.

10. Lock, R. C.: Test Cases for Numerical Methods in Two-Dimensional Transonic Flows. AGARD R-575-70. 1971.

11. Oswatitsch, Klaus: Gas Dynamics. Academic Press, Inc., 1956.

12. Hemenover, Albert D.: The Effects of Camber on the Variation With Mach Number of the Aerodynamic Characteristics of a 10-Percent-Thick Modified NACA Four-Digit-Series Airfoil Section. NACA TN 2998, 1953.

13. Nitzberg, Gerald E.; Crandall, Stewart M.; and Polentz, Perry P.: A Preliminary Investigation of the Usefulness of Camber in Obtaining Favorable Airfoil – Section Drag Characteristics at Supercritical Speeds. NACA RM A9G20, 1949.

14. von Kármán, T.: On the Foundation of High Speed Aerodynamics. Section A of General Theory of High Speed Aerodynamics. Vol. VI of High Speed Aerodynamics and Jet Propulsion, Princeton Univ. Press, 1954, p. 24.

15. Shapiro, Ascher H.: The Dynamics and Thermodynamics of Compressible Fluid Flow. The Ronald Press Co. N.Y. 1954.

16. Cole, Julian D.: Twenty Years of Transonic Flow. Paper presented at AIAA Meeting in San Francisco, June 16, 1969. Also D1-82-0878 Flight Sciences Lab. Boeing Scientific Res. Labs., 1969.

17. Knechtel, Earl D.: Experimental Investigation at Transonic Speeds of Pressure Distributions Over Wedge and Circular-Arc Airfoil Sections and Evaluation of Perforated-Wall Interference. NASA TN D-15, 1959.

18. Stanewsky, E.; and Little, B. H., Jr.: Studies of Separation and Reattachment in Transonic Flow. AIAA Paper 70-541, 1970.

19. Albert, I. E., Bacon, J. W., and Masson, B.S., and Collins, D. J., AIAA Paper 71-565, 1971.

20. Kutler, Paul; and Lomax, Harvard: Shock-Capturing, Finite-Difference Approach to Supersonic Flows. J. Spacecraft and Rockets, vol. 8, no. 12, Dec. 1971, p. 1175-1182.

21. Lighthill, M. J.: Higher Approximations. Section E of General Theory of High Speed Aerodynamics. Vol. VI of High Speed Aerodynamics and Jet Propulsion, Princeton Univ. Press, 1954, p. 414.

22. Ames Research Staff: Equations, Tables, and Charts for Compressible Flow. NACA Rep. 1135, 1953.

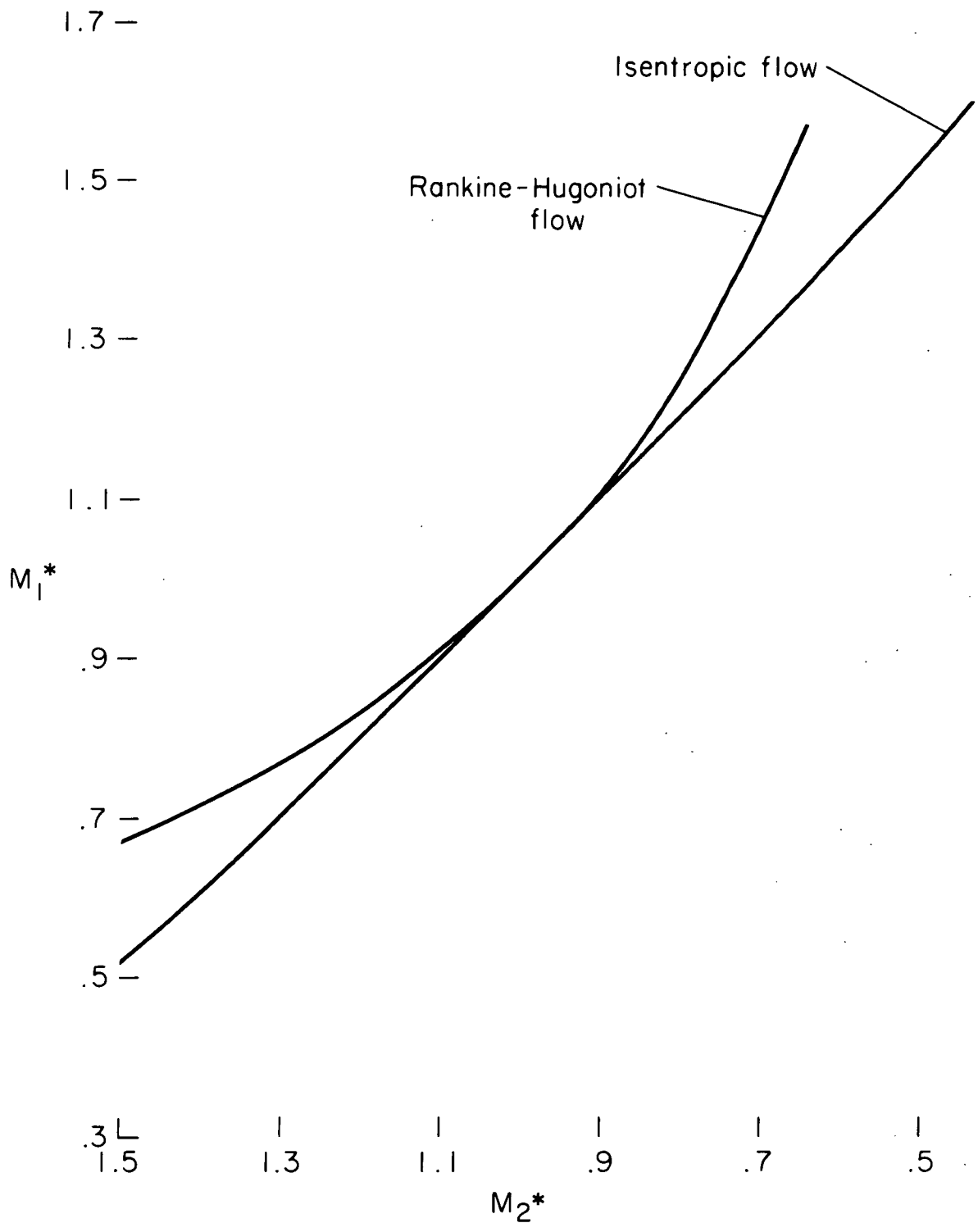

Figure 1. – Jump relations for normal shock.

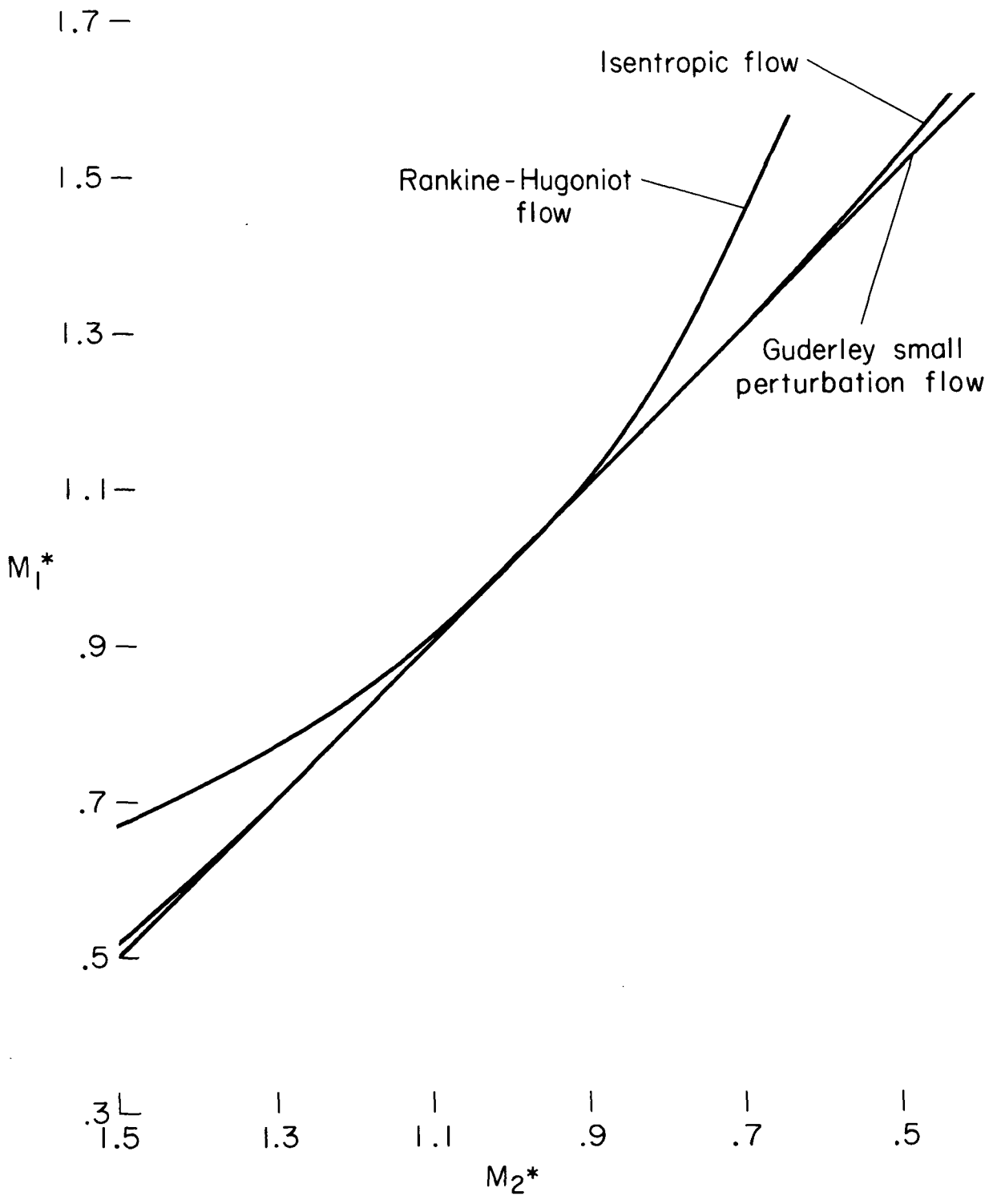

Figure 2. – Jump relations of Guderley's equation.

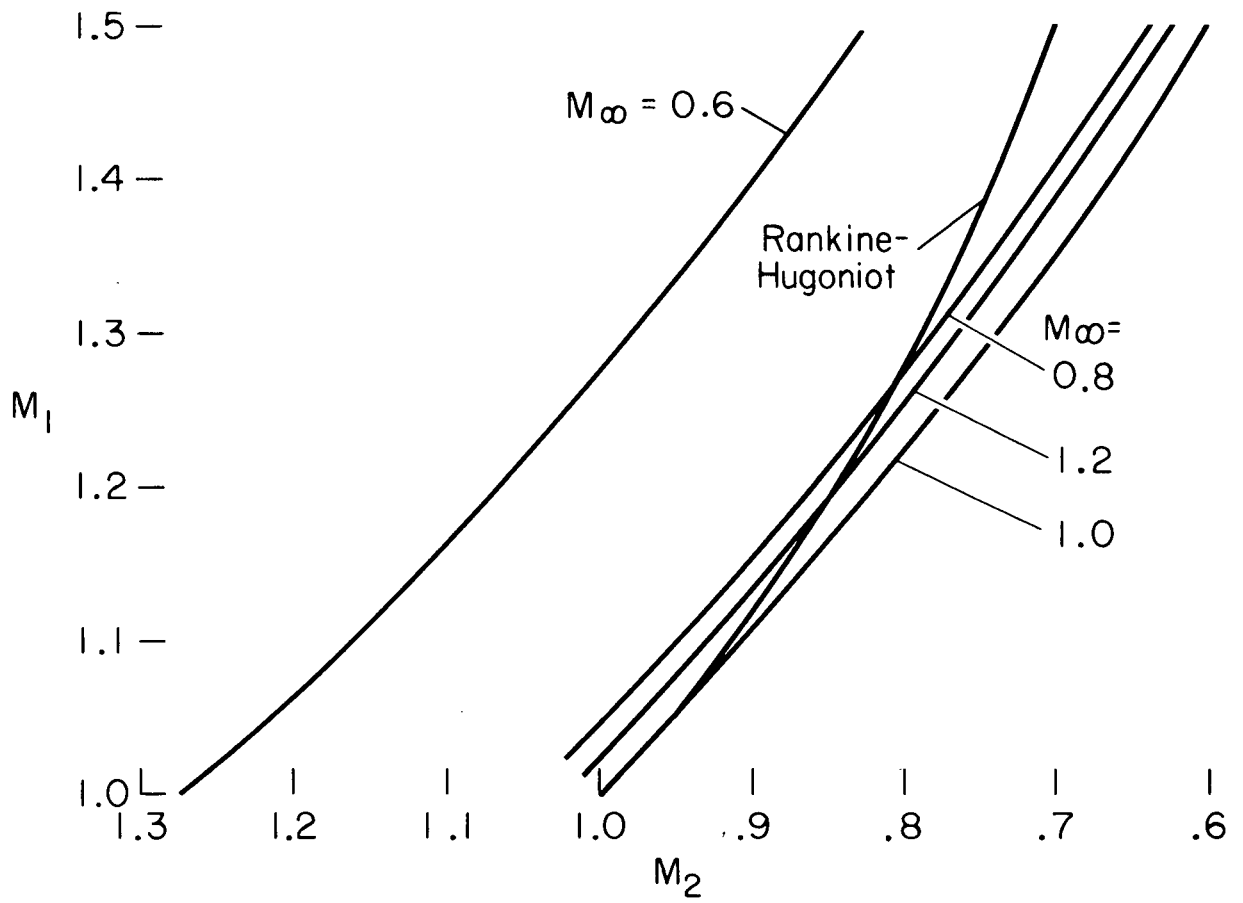

Figure 3. – Jump relations of Spreiter's equation.

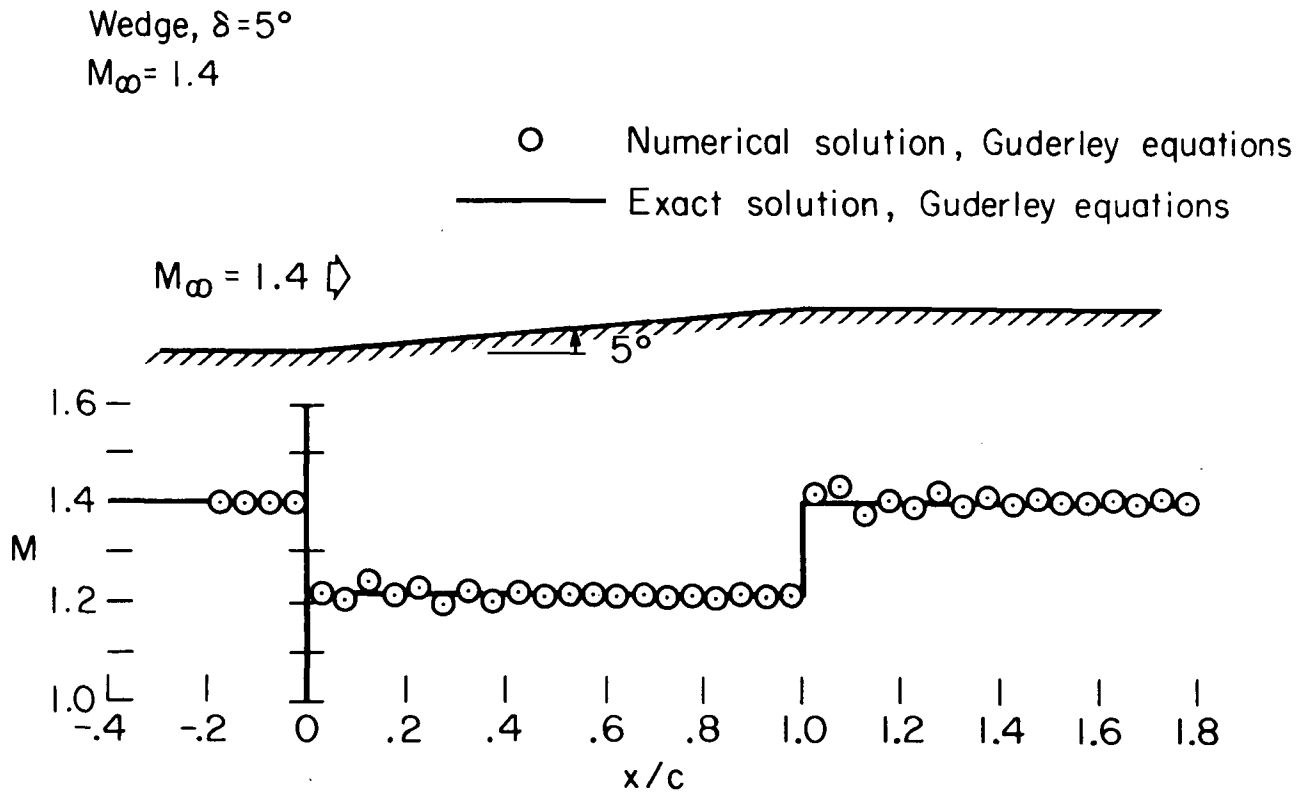

Figure 4. – Wedge flow solution, supersonic flow.

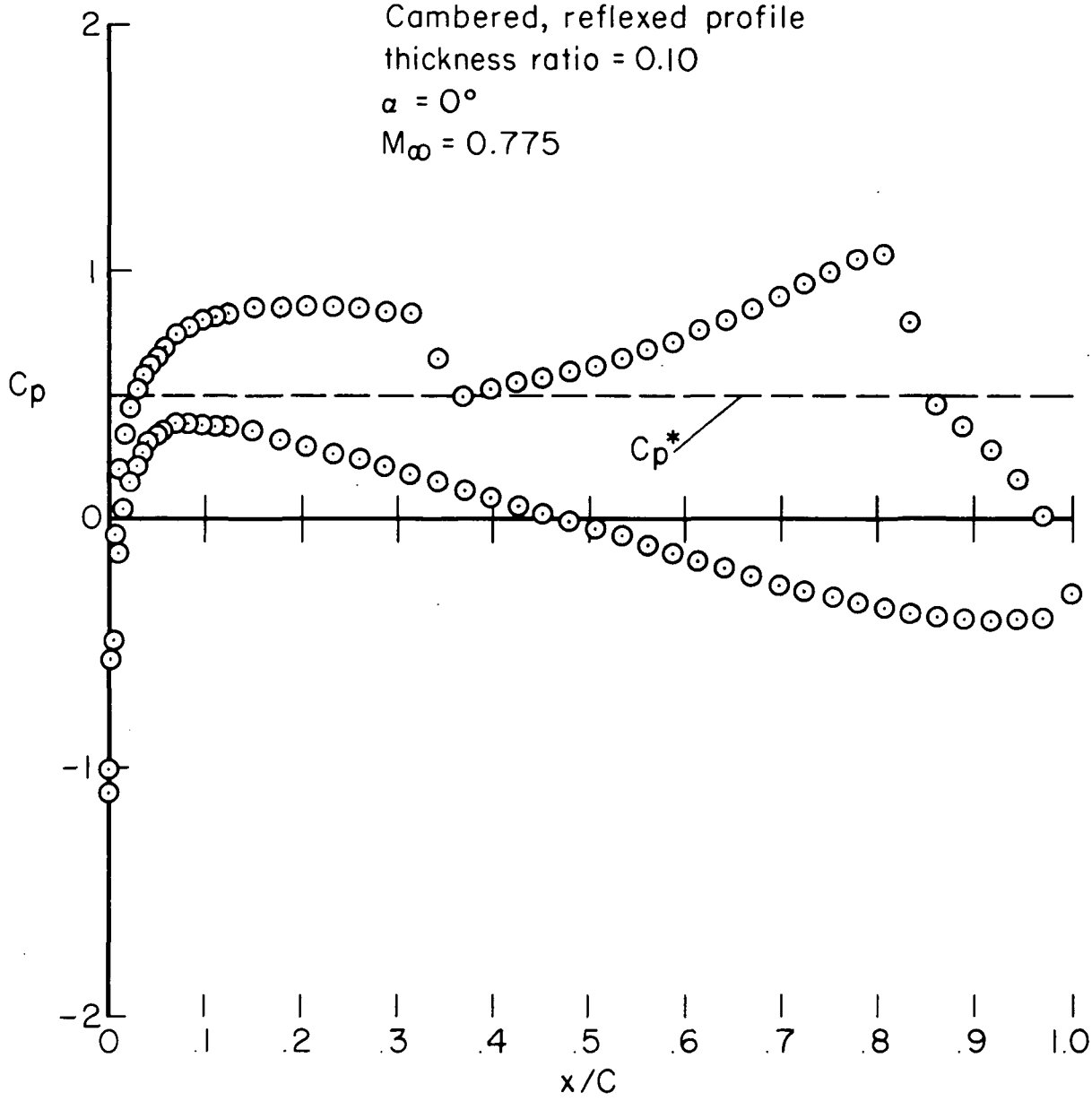

Figure 5. – Multiple shocked flow.

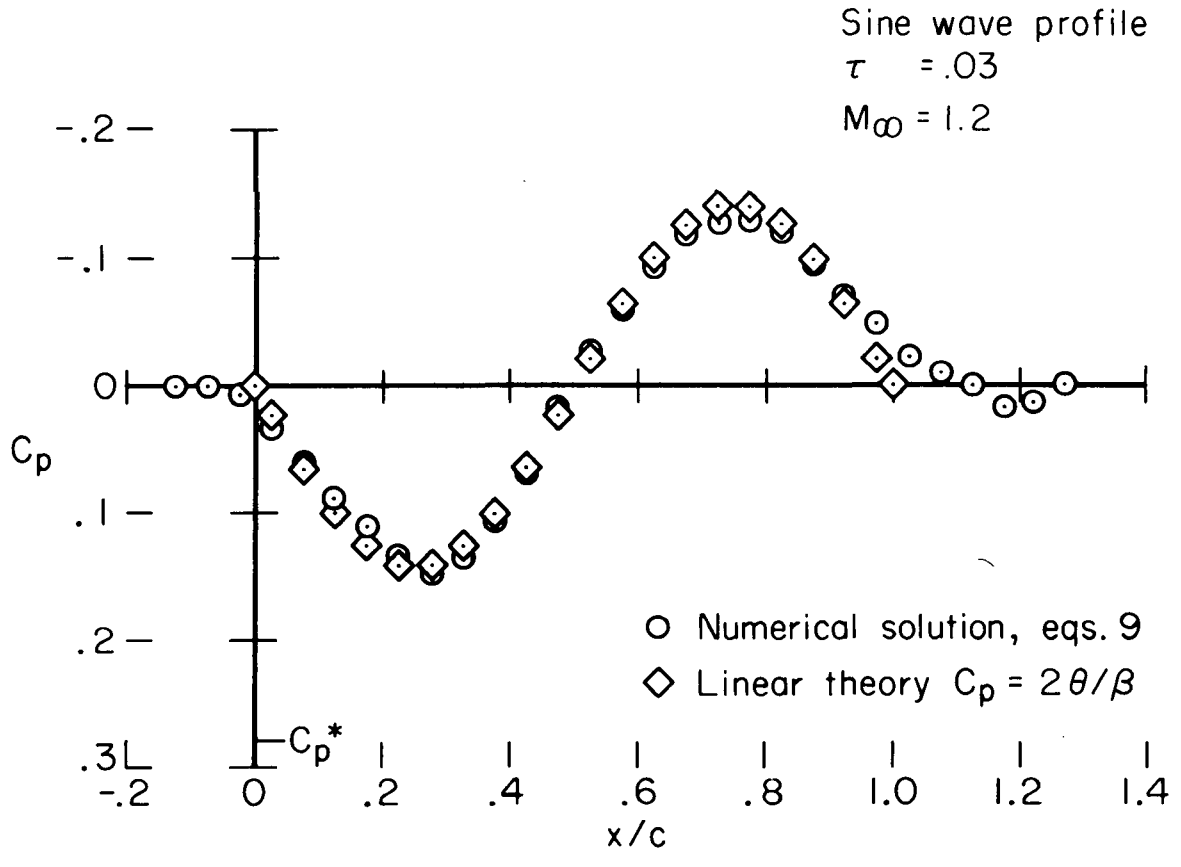

Figure 6. – Supersonic flow without surface shocks.

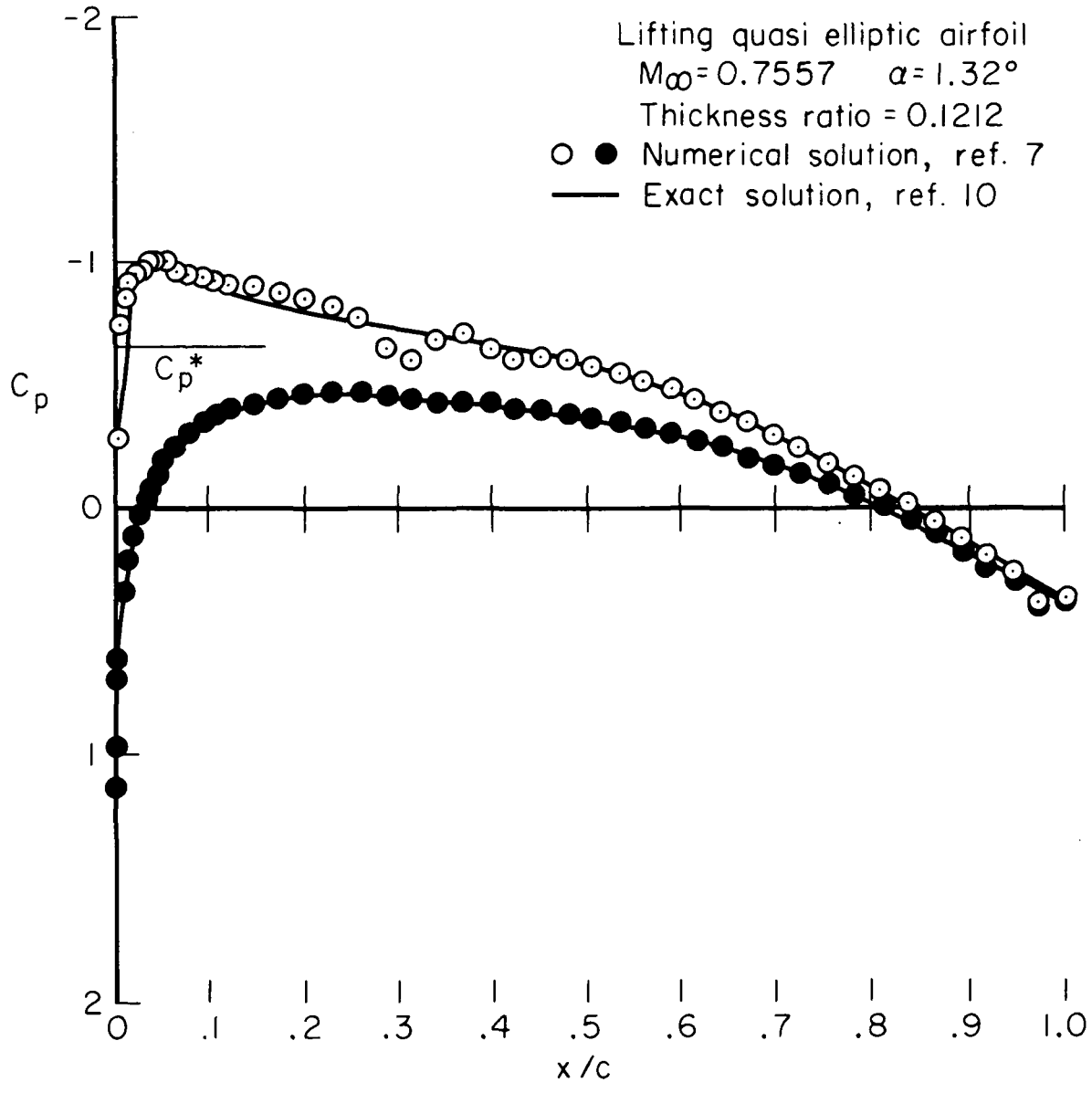

Figure 7. – Transonic flow for shock-free airfoil.

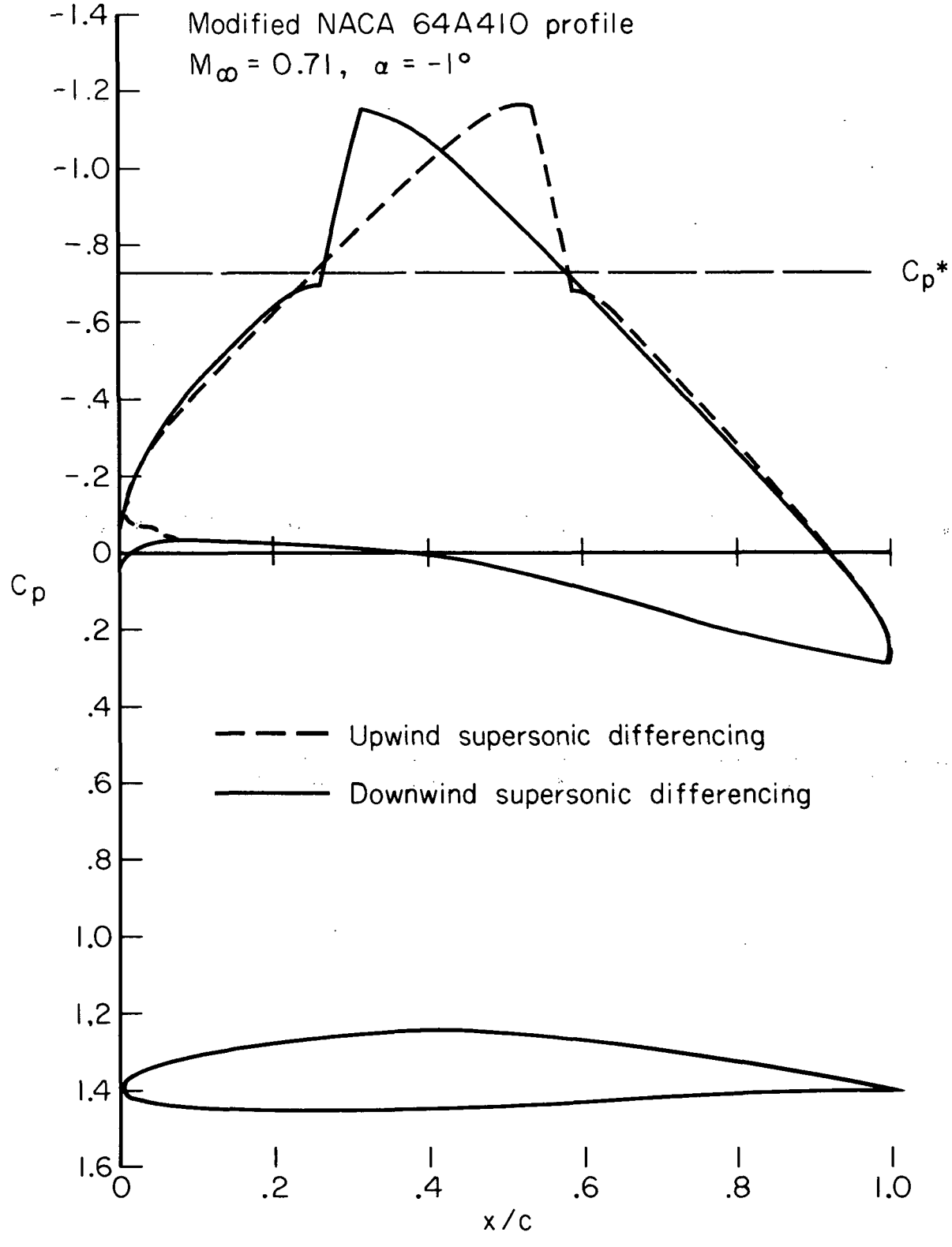

Figure 8. – Expansion shock solution compared to compression shock solution.

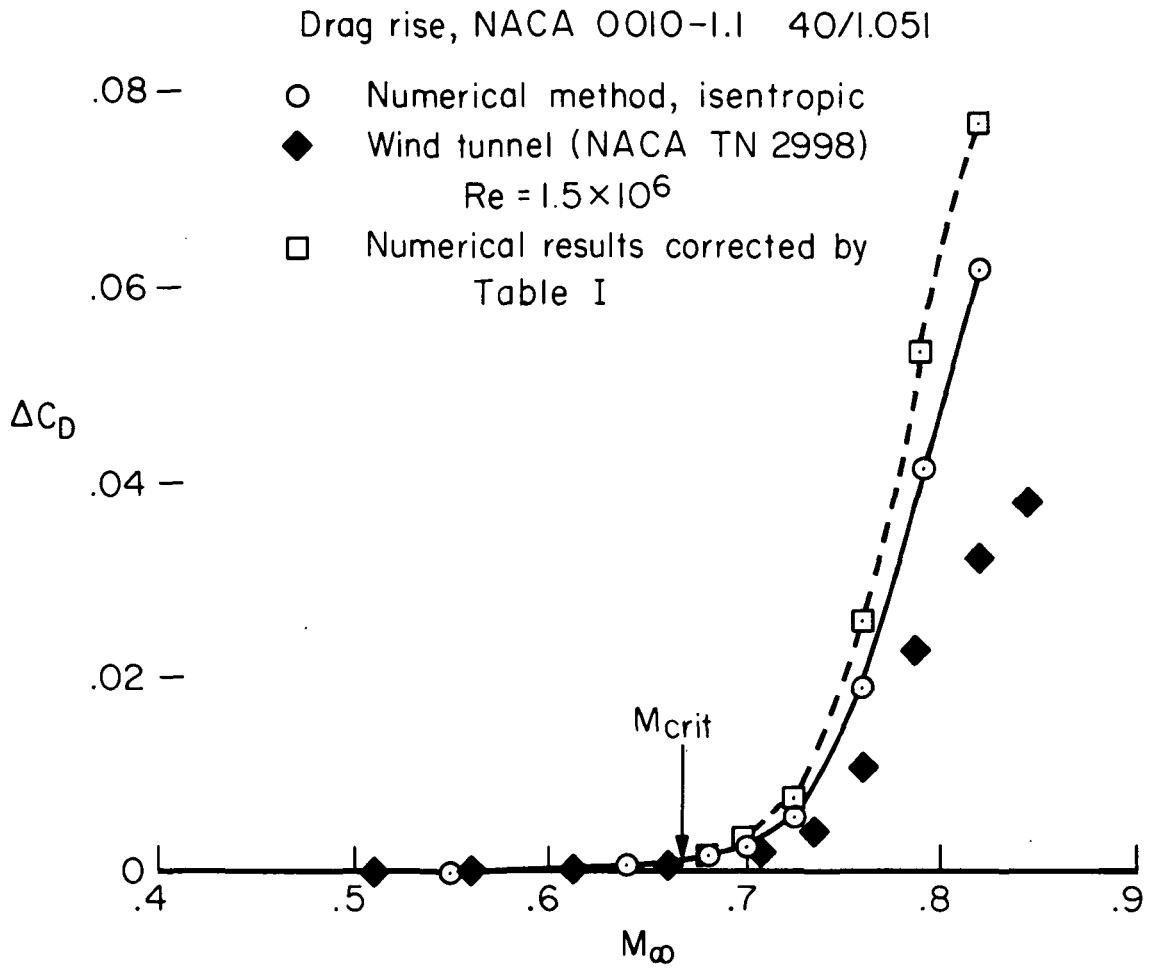

(a) Cambered.

Figure 9.– Drag rise for NACA 0010 profile.

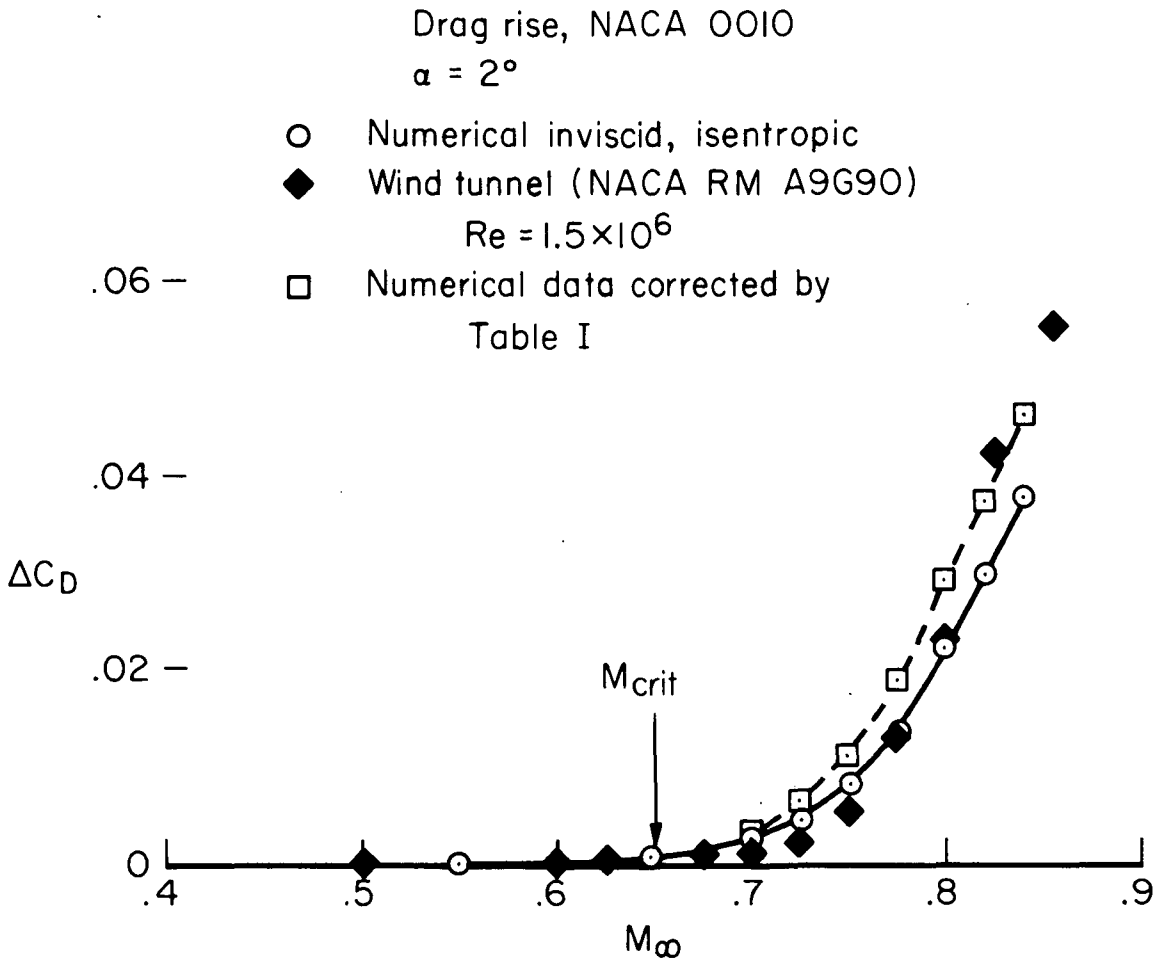

(b) 2° angle of attack.

Figure 9.– Concluded.

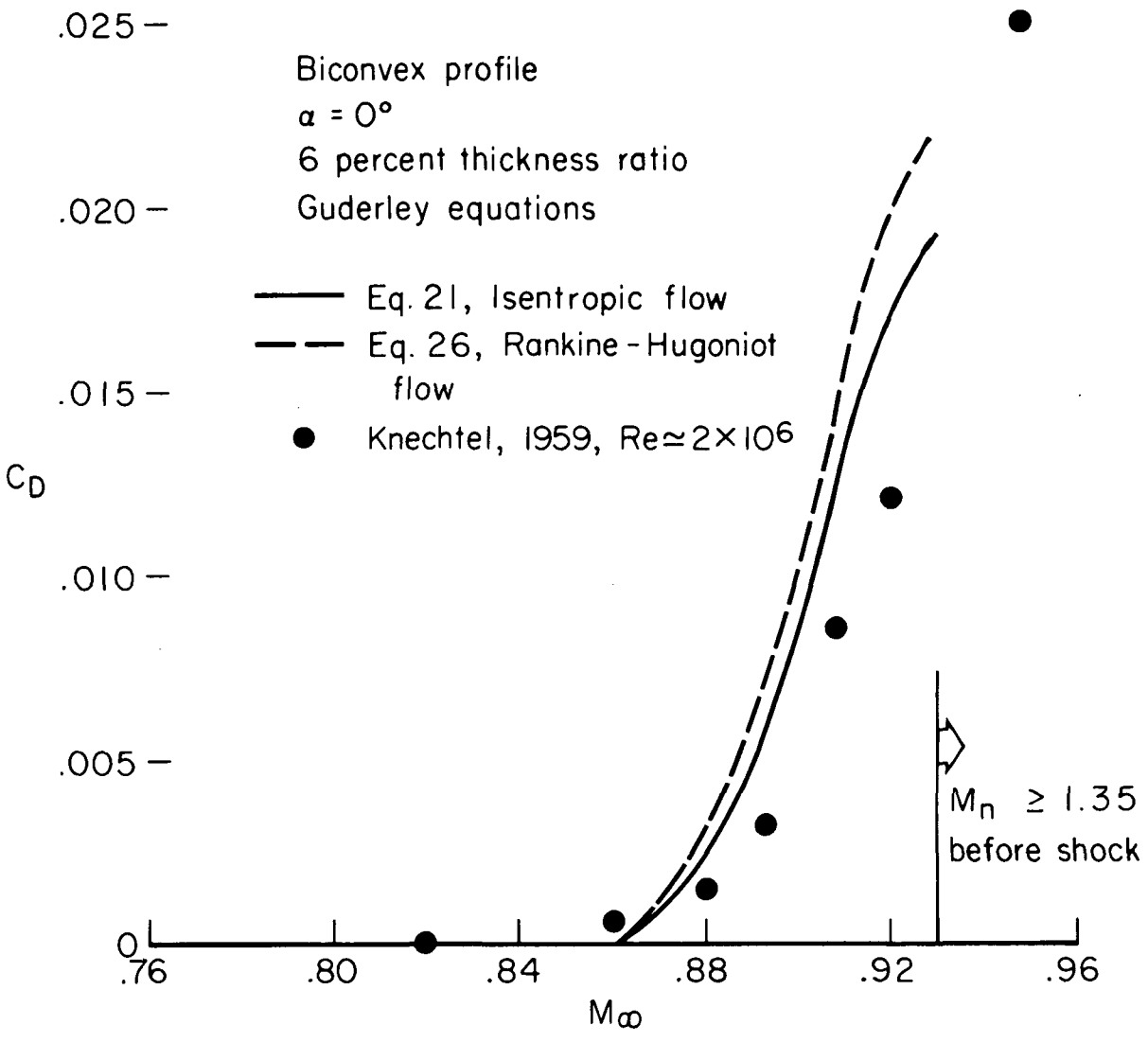

Figure 10. – Drag rise based on shock integration method.

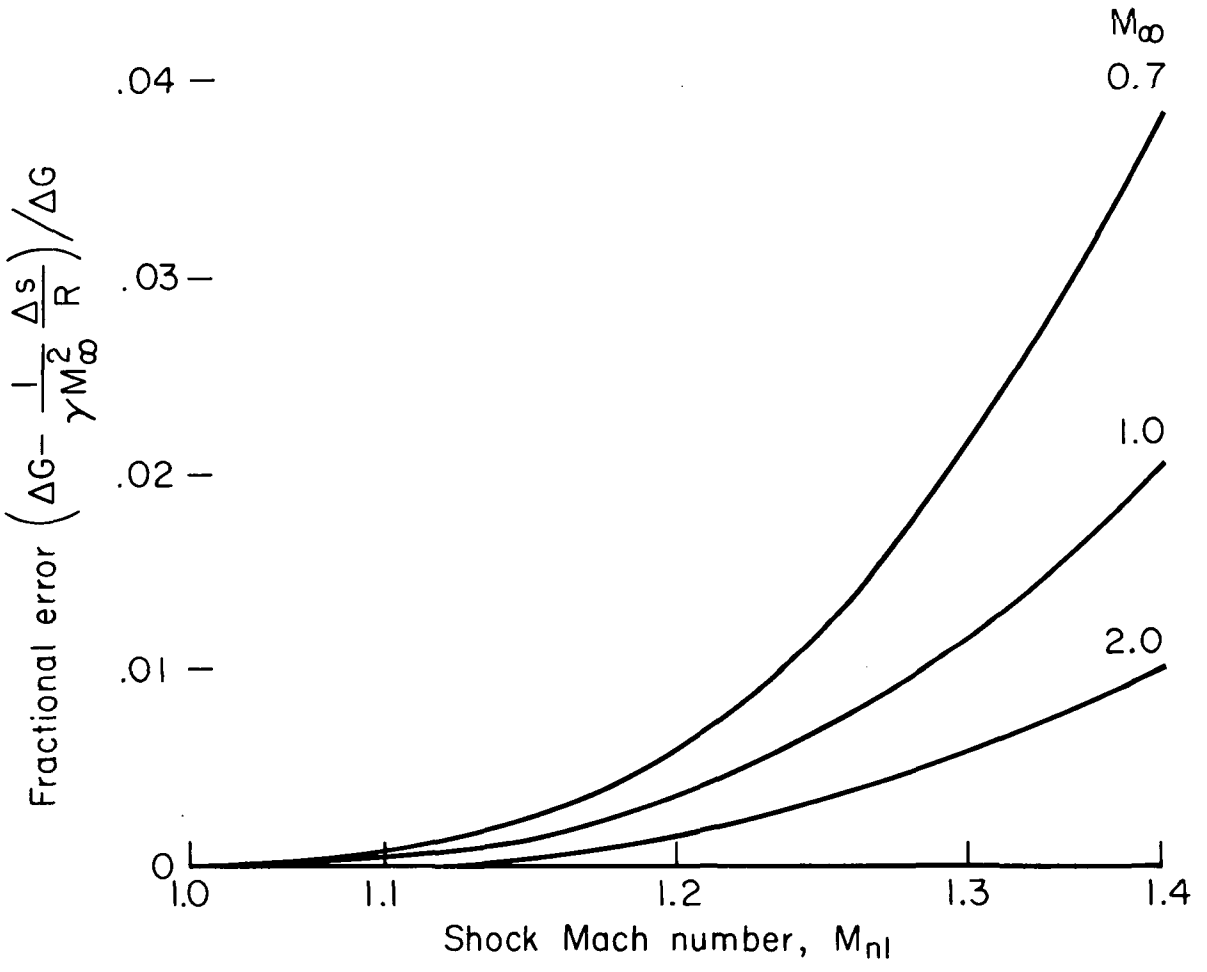

Figure 11. – Fractional error of Oswatitsch drag relation.

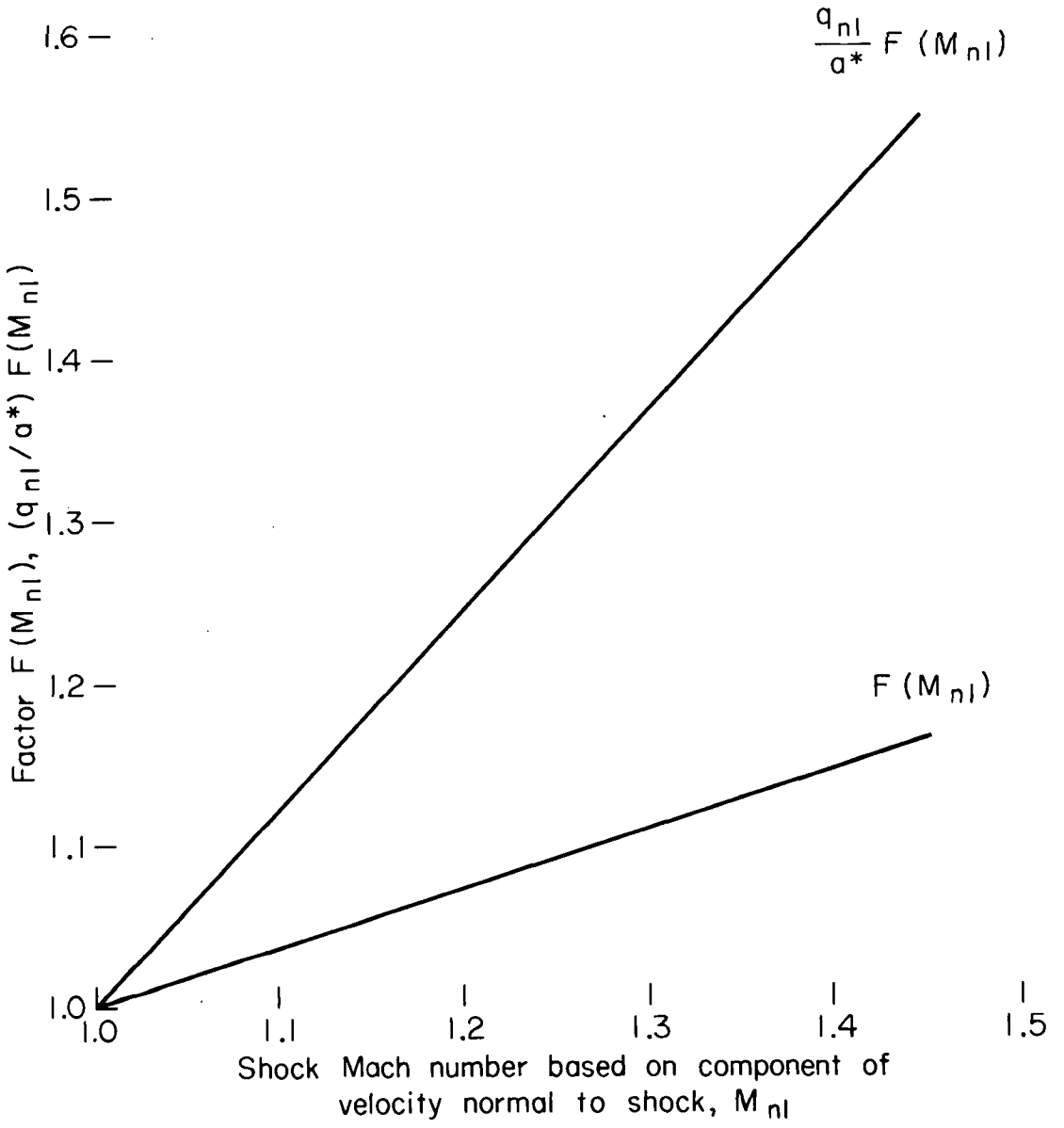

Figure 12. – Factors entering into the relationship between drags resulting from Rankine-Hugoniot and isentropic shock waves.

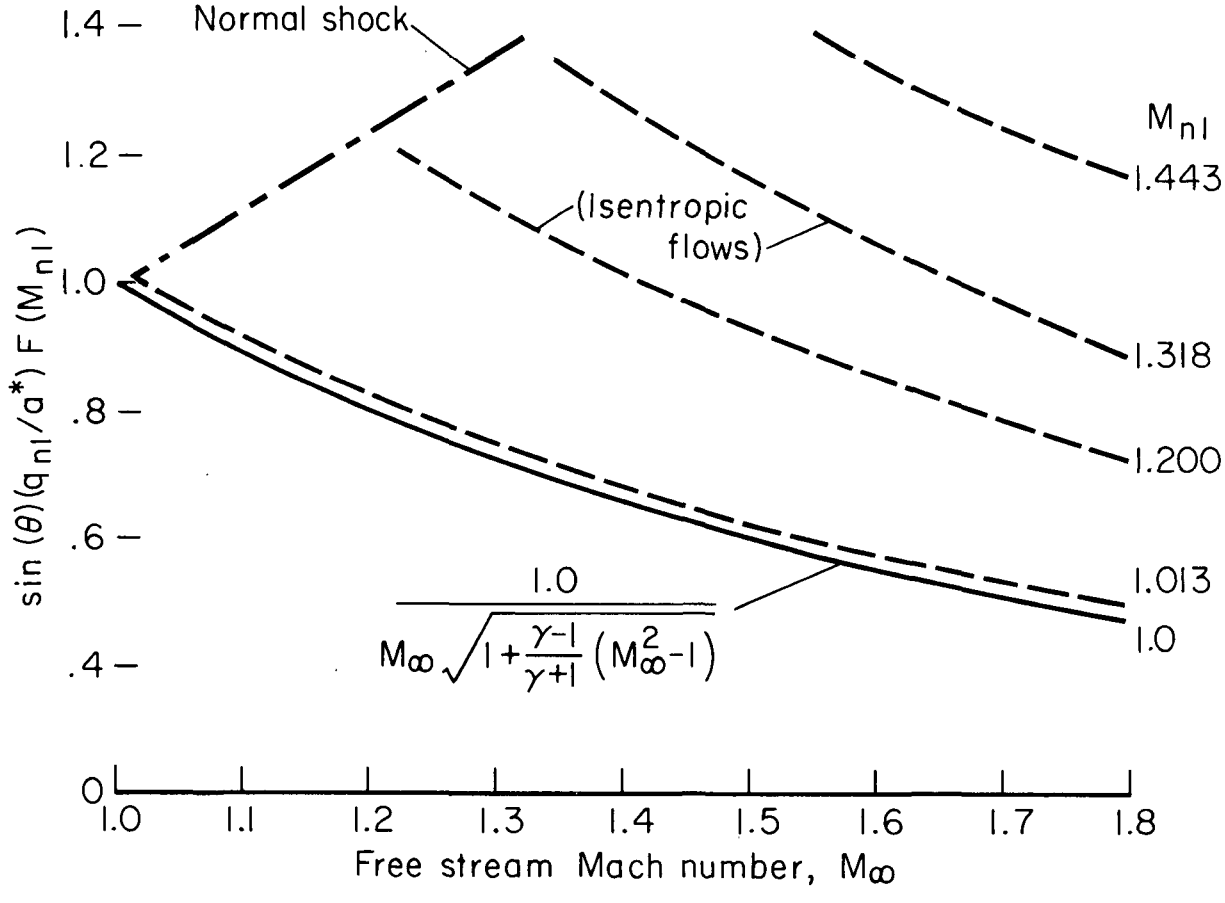

Figure 13. – Factor in equation (18) (isentropic flows) for oblique shock in supersonic free stream.

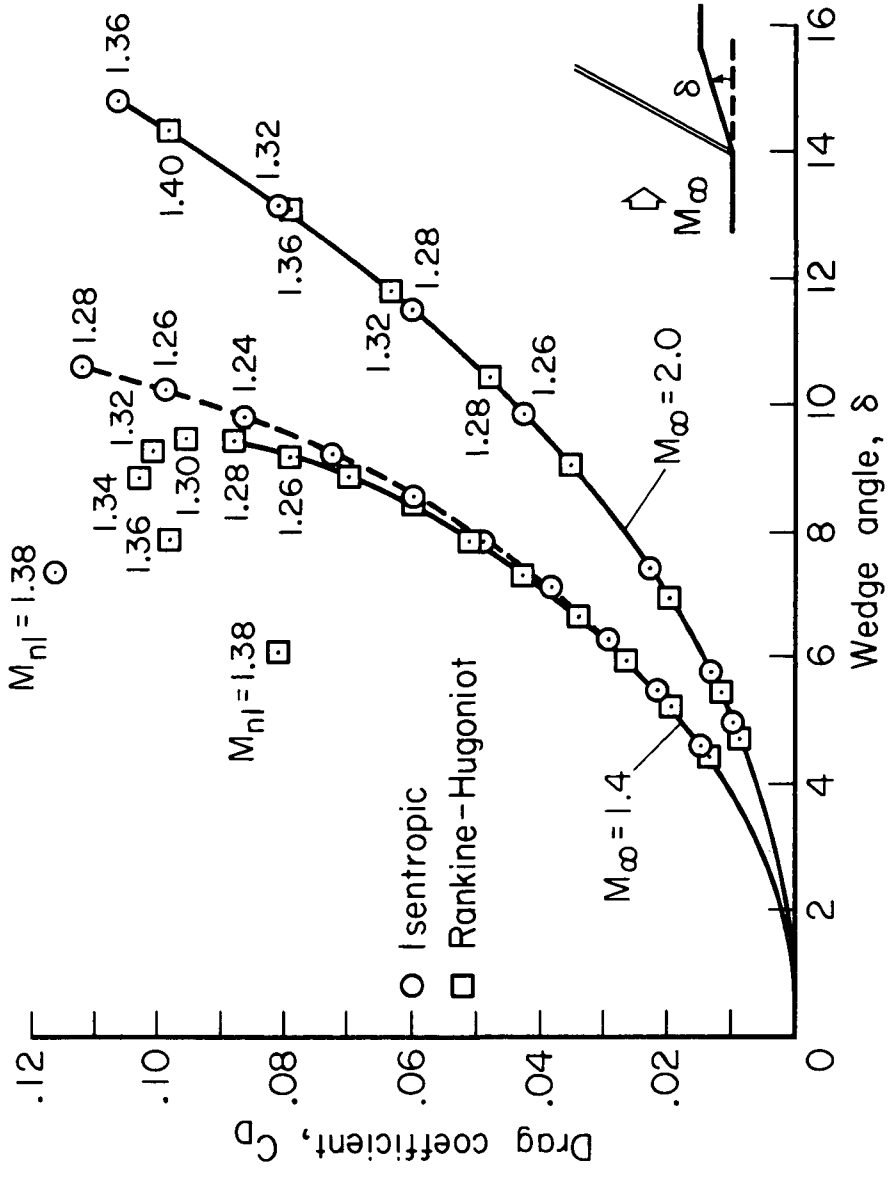

Figure 14. – Drag coefficients for a wedge in supersonic flow with Rankine-Hugoniot and isentropic shock waves.

NATIONAL AERONAUTICS AND SPACE ADMINISTRATION
WASHINGTON, D.C. 20546

OFFICIAL BUSINESS
PENALTY FOR PRIVATE USE $300

SPECIAL FOURTH-CLASS RATE BOOK

POSTAGE AND FEES PAID
NATIONAL AERONAUTICS AND SPACE ADMINISTRATION
451

U.S.MAIL

POSTMASTER: If Undeliverable (Section 158 Postal Manual) Do Not Return

"The aeronautical and space activities of the United States shall be conducted so as to contribute . . . to the expansion of human knowledge of phenomena in the atmosphere and space. The Administration shall provide for the widest practicable and appropriate dissemination of information concerning its activities and the results thereof."

—NATIONAL AERONAUTICS AND SPACE ACT OF 1958

NASA SCIENTIFIC AND TECHNICAL PUBLICATIONS

TECHNICAL REPORTS: Scientific and technical information considered important, complete, and a lasting contribution to existing knowledge.

TECHNICAL NOTES: Information less broad in scope but nevertheless of importance as a contribution to existing knowledge.

TECHNICAL MEMORANDUMS: Information receiving limited distribution because of preliminary data, security classification, or other reasons. Also includes conference proceedings with either limited or unlimited distribution.

CONTRACTOR REPORTS: Scientific and technical information generated under a NASA contract or grant and considered an important contribution to existing knowledge.

TECHNICAL TRANSLATIONS: Information published in a foreign language considered to merit NASA distribution in English.

SPECIAL PUBLICATIONS: Information derived from or of value to NASA activities. Publications include final reports of major projects, monographs, data compilations, handbooks, sourcebooks, and special bibliographies.

TECHNOLOGY UTILIZATION PUBLICATIONS: Information on technology used by NASA that may be of particular interest in commercial and other non-aerospace applications. Publications include Tech Briefs, Technology Utilization Reports and Technology Surveys.

Details on the availability of these publications may be obtained from:

SCIENTIFIC AND TECHNICAL INFORMATION OFFICE

NATIONAL AERONAUTICS AND SPACE ADMINISTRATION

Washington, D.C. 20546